Received: 13 October 2021 | Revised: 29 January 2022 | Accepted: 14 February 2022

DOI: 10.1049/cth2.12267

IET Control Theory & Applications

The Institution of Engineering and Technology WILEY

ORIGINAL RESEARCH PAPER

Fuzzy adaptive observer-based fault estimation design with adjustable parameter for satellite under unknown actuator faults and perturbations

Yanbo Li[1,2,3] | **Wei Xu**[1,3] | **Lin Chang**[1,3]

[1]Changchun Institute of Optics, Fine Mechanics and Physics, Chinese Academy of Sciences, Changchun, Jilin, China

[2]University of Chinese Academy of Sciences, Beijing, China

[3]Key Laboratory of Space-based Dynamic and Rapid Optical Imaging Technology, Chinese Academy of Sciences, Changchun, Jilin, China

Correspondence
Wei Xu, Changchun Institute of Optics, Fine Mechanics and Physics, Chinese Academy of Sciences, Changchun, Jilin 130033, China.
Email: xwciomp@126.com

Funding information
the National Natural Science Foundation of China, Grant/Award Number: 62005275

Abstract

This study considers the problem of fault estimation for rigid satellite in the presence of external disturbances, parameter perturbations, and actuator time-varying faults. Firstly, a Takagi-Sugeno (T-S) fuzzy model with interval matrix for satellite attitude system under large attitude angle scope is established, along with a detailed analysis of actuator faults in terms of additive and multiplicative descriptions. Then, a novel fuzzy adaptive observer with adjustable parameter is proposed to estimate both system states and actuator faults. The estimated errors are proved to be uniformly ultimately bounded, based on descriptor augmentation technique and Lyapunov stability theory. The proposed observer realizes a lower estimation performance index in terms of quantitative assessment compared to existing observer methods. Furthermore, an auxiliary optimization variable and the elimination method are applied to decrease the conservatism of the proposed design. And an intuitive quantitative performance index of fault estimation is introduced to obtain reliable evaluation and decision. Finally, numerical simulations and analyses of rigid satellite illustrate the effectiveness and benefit of the proposed strategy.

1 | INTRODUCTION

For remote sensing satellites, attitude manoeuvres with actuator faults could lead to the failure of observation missions due to the unexpected behaviour and degraded stability. In order to strengthen system stability and maintainability, as well as to lower the operating cost, timely fault estimation and fault-tolerant control schemes of the satellite attitude system are developed to maintain desired performance and stability even when faults occur [1–4]. Hence, the research on fault estimation to ensure the long-term normal operation of satellite has obtained considerable attention.

Adaptive observer is widely used in fault diagnosis due to its simple structure, strong practicability and the ability that is able to estimate system state and fault simultaneously [5–7]. Adaptive observer-based fault estimation is applied to acquire accurate fault information by reconstructing the magnitude of faults [8–10]. However, there is a strict equality constraint in the adaptive observer design, which makes it more difficult to calculate design parameters. To overcome the restriction of the observer matching condition, an intermediate estimator strategy is developed by introducing one or more intermediate variables in [11], which does not require the strict equality constraint and is proved that estimation errors of system state and fault are ultimately uniformly bounded. Furthermore, there are model uncertainties in the actual satellite attitude system inevitably, including modelling errors, parameter perturbations and external disturbances [12–14]. Specifically, a small variation of parameter may have a great effect on the fault estimation results after an amplification of a large adaptive gain or learning rate [15]. Therefore, compared with constant system parameters, the influence of parameter perturbation on fault estimation deserves more attention. Under the circumstances, some researches introduce augmentation idea to strengthen the application field of adaptive observer [16–18]. In [1], with the consideration of Lipschitz nonlinearity and external disturbance, a sensor fault estimation method of rigid satellite is discussed, where the sensor fault is regarded as an augmented state. In

[19, 20], based on H_∞ performance index, adaptive observers with adjustable parameters are designed for continuous/discrete dynamic systems and a class of nonlinear interconnected systems, which can obtain more design freedoms and a lower fault estimation performance index in comparison with the conventional augmented observer design. The design of suppressing synthetic disturbances mentioned above can be similarly found in [21, 22]. Ref. [23] investigates two unknown input observers to deal with the fault diagnosis problem for nonlinear systems with Lipschitz nonlinearities, where the disturbances effects are attenuated by dissipativity theory. In [24], actuator faults, external disturbances, and uncertain inertia parameter of a rigid spacecraft are regard as a lumped disturbance together, which is estimated via a finite-time disturbance observer. Considering the coupling effect between the observer error dynamics and the control system, an H_∞ based adaptive observer is developed for nonlinear Lipschitz systems in the presence of external disturbances and actuator faults [25]. More results on the fault diagnosis including the quantitative and qualitative methods for continuous-time systems and discrete-time systems can be found in [26].

One of the key challenges of fault estimation observer in the rigid satellite comes from their strong non-linearity and high uncertainty. In [5], with new state variables corresponding to the integrated output variables, the augmented satellite attitude system model uses adaptive observers to obtain fault estimation of actuator and sensor faults. A nonlinear geometric approach is utilized to avoid the unwanted influence on the fault estimates caused by aerodynamic disturbance torques. Similarly, an adaptive observer is designed for the actuator and sensor faults estimation based on augmented model with unmeasurable premise variables [27]. Where a new state is applied that is a filtered version of output variables. Meanwhile, learning observer strategy has been considered in some researches, and considerable discussions have been conducted on the fault estimation of satellite attitude system [28, 29]. Compared with [29], the iterative learning observer in [28] has stronger robustness with respect to external disturbances by introducing a switch term. All the results mentioned above are based on the premise that the satellite inertia matrix is known and constant. In [30], the rigid satellite attitude system with sensor faults and uncertainties is transformed into two subsystems: the sensor faults exist in subsystems-2 and uncertainties are in subsystems-1, where the satellite is assumed to work in small attitude angles. The sensor faults are estimated by an adaptive observer, and the design parameters of the observer are resolved by using linear matrix inequality (LMI) techniques. In [31], an adaptive sliding mode fault estimation observer is designed to acquire the estimated value of unknown time-varying faults, where the attitude angles of rigid satellite are assumed to vary in a small range. The same assumption constraint for rigid satellites can also be found in [1]. However, the large attitude angle working scope is inevitable, especially for advanced satellites with the requirement of rapid mobility, such as Worldwiew-2 [32], JL-1 smart verification satellite [33], and optical conical scanning imaging small satellites [34]. How to further carry out fault estimation of satellite attitude system under large angle manoeuvre is an interesting issue and motivates our study.

Over the past three decades, Takagi-Sugeno (T-S) fuzzy model and control strategy have verified to be a very powerful and flexible tool to cope with non-linear systems. By using a set of locally linearized dynamics connected by fuzzy membership functions, T-S fuzzy models have the ability to approximate the complicated non-linear behaviours of dynamics with any specified accuracy [35]. The design of controller and observer for T-S fuzzy models can be represented in terms of LMI [36–38]. Based on linear switching function and integral-type switching function, [39] provides two design methods for the T-S fuzzy descriptor sliding mode observer. Ref. [40] deals with a memory integral sliding-mode control problem for the permanent magnet synchronous motor model with mismatched disturbance based on disturbance observer and T-S fuzzy approach. In [41], a T-S fuzzy functional observer is investigated to detect the fault for fuzzy systems with time-delay and exogenous disturbance. Actually, considering the large attitude angle motion process of satellite with multiple disturbances, T-S fuzzy approach provides a new opportunity for achieving the fault estimation observer design.

Motivated by the discussions earlier, in this paper, the satellite attitude system with model uncertainties is approximated by the T-S fuzzy models, which can be applied to manoeuvring at any angle. Then, a fuzzy adaptive fault estimation observer (FAFEO) with adjustable parameter (AP) is designed for the non-linear satellite system, which combines multivariable optimization design with fuzzy adaptive observer to address the problem of actuator fault estimation, under model uncertainties above mentioned. It should be pointed out that, reviewing the existing fault estimation methods, the fault estimation method applied to general satellite attitude system (considering the model uncertainties, no manoeuvre angle constraints) is less considered. Based on Lyapunov methodology and H_∞ theory, the proposed method is able to guarantee that the dynamic error system is asymptotically stable and estimation errors are ultimately uniformly bounded. The proposed scheme is analytically verified and illustrated via numerical simulation results. The main contributions of this work are summarized as follows:

1. Presented fault estimator with adjustable parameter is designed as a proportional-integral (PI) function of angular velocity estimation error. The proposed method can not only provide additional design freedom to the fuzzy adaptive observer but also enhance transient and steady-state performance of fault estimation. Particularly, the proposed method could find lower fault estimation performance index than existing methods [10, 15], while the computing complexity is not too much increased.
2. The proposed scheme is given in the form of LMI, with less conservatism as well as retaining the performance of the proposed algorithm. By introducing an auxiliary index on H_∞ optimization, the stability condition of observer system can be relaxed. Moreover, the strong assumption of common Lyapunov matrix considered in [19, 20] is relaxed. Based on the elimination method, the strict implicit constraint in the

sufficient existence condition of observer design with pole placement is eliminated, which leads to a larger feasible area of stabilization than Theorem 3 given in [19].

This paper is organized as follows. The dynamic model for satellite attitude system with actuator faults is established in Section 2. Section 3 shows a novel FAFEO with AP to achieve online fault estimation, where some relaxation strategies are presented. Section 4 gives the simulation results, which verify the effectiveness of the proposed strategy. In Section 5, conclusions of this paper is drawn.

2 | PROBLEM FORMULATION

The following notations are used. A^T represents the transpose form of the matrix A; $\langle A\rangle_S$ represents the form $A + A^T$; * is used for blocks induced by symmetry; $diag(\cdot)$ denotes the block diagonal matrix; I denotes the identity matrix with appropriate dimensions; $\|\cdot\|_p$ denotes the p-norm in the Euclidean space; $\bar{\sigma}(\cdot)$ denotes the maximum singular value of a matrix.

In this study, the attitude motion model of a rigid satellite with external disturbances can be given by [4, 28]

$$J\dot{\omega} + \omega^{\times} J\omega = u + u_d \tag{1}$$

$$\begin{aligned} \dot{q}_0 &= -\frac{1}{2} q_v^T \omega \\ \dot{q}_v &= \frac{1}{2}(q_0 I_3 + q_v^{\times})\omega \end{aligned} \tag{2}$$

where Equations (1) and (2) represent the dynamics subsystem and the kinematics subsystem, respectively. $J \in \mathbb{R}^{3\times3}$ is the satellite inertia matrix. $\omega^T = [\omega_x\ \omega_y\ \omega_z] \in \mathbb{R}^{1\times3}$ denotes the space rotation angular velocity of satellite, expressed in the body frame O_B relative to the inertial frame O_I. $u^T = [u_1\ u_2\ u_3] \in \mathbb{R}^{1\times3}$ is the expected control input and is constrained in a compact set, that is, $|u| < u_{\max}$, where $u_{\max}$ is a positive constant. $u_d \in \mathbb{R}^{3\times1}$ is the external environmental disturbance torque, including the air drag, solar radiation pressure and gravity gradient moment [4, 5]. $q = [q_0\ q_v^T] \in \mathbb{R}^{4\times1}$, satisfying the constraint $\|q\|_2 = 1$, is the unit quaternion representing the attitude orientation of the satellite in O_B with respect to O_I. $w^{\times}(w = q_v, \omega)$ is the cross product operator for $w^T = [w_1\ w_2\ w_3] \in \mathbb{R}^{1\times3}$ described by

$$w^{\times} = \begin{bmatrix} 0 & -w_3 & w_2 \\ w_3 & 0 & -w_1 \\ -w_2 & w_1 & 0 \end{bmatrix}$$

Considering control issues of attitude tracking and holding, the attitude tracking error $q_e = (q_{e0}, q_{ev}^T) \in \mathbb{R}^{4\times1}$ is defined to characterize the relative orientation between O_B and the desired frame O_D. Giving the desired satellite attitude $q_d = (q_{d0}, q_{dv}^T) \in \mathbb{R}^{4\times1}$, (q_{e0}, q_{ev}^T) is computed by

$$\begin{bmatrix} q_{e0} \\ q_{ev} \end{bmatrix} = \begin{bmatrix} q_{dv}^T q_v + q_{d0} q_0 \\ q_{d0} q_v - q_{dv}^{\times} q_v - q_{dv} q_0 \end{bmatrix} \tag{3}$$

where $\|q_e\|_2 = 1$ and $\|q_d\|_2 = 1$.

Similarly, we define the angular velocity tracking error $\omega_e \in \mathbb{R}^{3\times1}$ as

$$\begin{aligned} \omega_e &= \omega - \Theta_q \omega_d \\ \Theta_q &= \left(q_{e0}^2 - q_{ev}^T q_{ev}\right) I_3 + 2 q_{ev} q_{ev}^T - 2 q_{e0} q_{ev}^{\times} \end{aligned} \tag{4}$$

where ω_d is desired attitude angular velocity, Θ_q is the rotation matrix.

On the basis of above tracking errors, we define the controller input variable $s_e \in \mathbb{R}^{3\times1}$ as

$$s_e = q_e + \beta \omega_e \tag{5}$$

where $\beta > 0$ is a given constant.

The following classical proportional-integral-derivative (PID) control scheme is implemented:

$$u = k_p s_e + k_i \int s_e dt + k_d \frac{d s_e}{dt} \tag{6}$$

where k_p, k_i, k_d are the proportional term, integral term, and derivative term, respectively.

Apart from the above, two important problems deserving more attention are satellite inertia uncertainties ΔJ and actuator faults $f(t) \in \mathbb{R}^{3\times1}$. Replacing J with $J_0 + \Delta J$, the dynamics subsystem can be rewritten as

$$\dot{\omega} = -(J_0 + \Delta J)^{-1} \omega^{\times} (J_0 + \Delta J)\omega + (J_0 + \Delta J)^{-1}\left(u + f + u_d\right) \tag{7}$$

where J_0 is the normal part of inertia matrix, known and non-singular. ΔJ is an unknown matrix related to the mass displacement owing to the fuel consumption and drastic vibration during launch, or mounting misalignment [12]. In practice, $J_0 + \Delta J$ can remain bounded and non-singular as device physical limitations and mature engineering design.

Remark 1. The normal part of inertia matrix can be represented as:

$$J_0 = \begin{bmatrix} J_{11} & 0 & 0 \\ * & J_{22} & 0 \\ * & * & J_{33} \end{bmatrix} + \begin{bmatrix} 0 & J_{12} & J_{13} \\ * & 0 & J_{23} \\ * & * & 0 \end{bmatrix}$$

where J_0 is non-singular; J_{11}, J_{22}, and J_{33} are the triaxial moment of inertia; J_{12}, J_{13}, and J_{23} are products of inertia. Generally, from the perspective of engineering application, $J_{ii}(i = 1, 2, 3)$ are much larger than $J_{ij}(i < j; i = 1, 2; j = 2, 3)$, and J_{ii} are in the same order of magnitude. (1) As the inertia axis through

the centre of mass approaching the satellite body frame O_B, the inertia products J_{ij} become smaller, which will contribute to reduce the control coupling among axes. Ideally, the two frames coincide, that is, $J_{ij} = 0$. (2) Considering the gravity gradient torque d_G, satellites have the symmetrical mass distribution. When d_G is considered as the disturbance torque, as in this paper, it is necessary to make J_{ii} as equal as possible in the design of satellite. On the contrary, it is a good choice to appropriately increase the difference among J_{ii} when d_G is used as the attitude stability torque. (3) Under the current mature engineering design, the inertia uncertainties ΔJ is a relatively small quantity compared with J_0. Thus, $J_0 + \Delta J$ is still non-singular.

Remark 2. The actuator fault model could be summarized into the following form [28, 31].

$$u'(t) = \Pi_u u(t) + \Sigma_u$$

where $u'(t)$ denotes the actual driving torque. $\Pi_u = diag(\chi_1, \chi_2, \chi_3)$ denotes the fault condition of actuators in a multiplicative way with $0 \le \chi_i \le 1, i = 1, 2, 3$. The partial fault shows that the actual driving torque applied by the actuator to the satellite attitude system is less than the expected control input generated by the controller. Σ_u represents the fault condition in an additive way, such as, a time-varying torque independent of the expected control input continuously generated by the actuator, and a fixed actual driving torque due to the actuator is stuck in a fixed position. $\Pi_u = I_3$ and $\Sigma_u = 0$ only if no faults occur for all actuators, which indicates the actual driving torque is equivalent to the expected control input. Furthermore, here is the equivalent form $u'(t) = u(t) + \Sigma'_u$ with $\Sigma'_u = (\Pi_u - 1)u(t) + \Sigma_u$, which is to facilitate the design of following proposed observer.

According to matrix inversion formula [42], we have

$$(J_0 + \Delta J)^{-1} = J_0^{-1} - J_0^{-1}\Delta J\left(I + J_0^{-1}\Delta J\right)^{-1} J_0^{-1} \tag{8}$$

By substituting (8) into (7), system (7) becomes

$$\dot{\omega} = \left\{-J_0^{-1}\omega^{\times}J_0 + J_0^{-1}\left[\Delta J\left(I + J_0^{-1}\Delta J\right)^{-1} J_0^{-1}\omega^{\times}(J_0 + \Delta J) - \omega^{\times}\Delta J\right]\right\}\omega + \left\{J_0^{-1} - J_0^{-1}\Delta J\left(I + J_0^{-1}\Delta J\right)^{-1} J_0^{-1}\right\}(u + f + u_d) \tag{9}$$

Based on T-S fuzzy modelling approach, the dynamics subsystem (9) can be approximated by the following IF-THEN rules [35, 42].

Model rule i: IF $z_1(t)$ is M_1^i and … and $z_p(t)$ is M_p^i, THEN

$$\begin{cases} \dot{x}(t) = (A_i + \Delta A_i)x(t) + (B_i + \Delta B_i)\left(u(t) + f(t) + u_d(t)\right) \\ y(t) = C_i x(t) \end{cases}, \quad i = 1, 2, \ldots, r \tag{10}$$

$$A_i = -J_0^{-1}\omega^{\times}J_0,\ B_i = J_0^{-1},\ C_i = I$$

$$\Delta A_i = J_0^{-1}\left\{\Delta J\left(I + J_0^{-1}\Delta J\right)^{-1} J_0^{-1}\omega^{\times}(J_0 + \Delta J) - \omega^{\times}\Delta J\right\}$$

$$\Delta B_i = -J_0^{-1}\Delta J\left(I + J_0^{-1}\Delta J\right)^{-1} J_0^{-1}$$

where $z_j(t)(j = 1, 2, \ldots, p)$ are measurable premise variables; M_j^i is the fuzzy set and r is the number of model rules; $x(t) = [x_1(t)\ x_2(t)\ x_3(t)]^T$ is the system state with $x_1(t) = \omega_x(t)$, $x_2(t) = \omega_y(t)$, and $x_3(t) = \omega_z(t)$; $y(t)$ is the measurement output. In this study, we choose the state vector $x(t)$ as the premise variable $z(t)$, that is, $z_1(t) = \omega_x(t)$, $z_2(t) = \omega_y(t)$, and $z_3(t) = \omega_z(t)$. Then, there are common matrices $B_i = B = J_0^{-1}$, $\Delta B_i = \Delta B = -J_0^{-1}\Delta J(I + J_0^{-1}\Delta J)^{-1}J_0^{-1}$, and $C_i = C = I$. For the unmeasurable factor $(B + \Delta B)u_d(t)$, we consider that $B_d d(t) = (B + \Delta B)u_d(t)$ with distribution matrix $B_d = J_0^{-1}$. ΔA_i and ΔB represent the perturbation matrices caused by satellite inertia uncertainties. These matrices can be decomposed into the given form $[\Delta A_i\ \Delta B] = [D_a\Delta_{ai}E_a\ D_b\Delta_b E_b]$, where $D_a = \alpha_a J_0^{-1}$, $E_a = \alpha_a^{-1}I_3$, $D_b = -\alpha_b J_0^{-1}$, and $E_b = \alpha_b^{-1}J_0^{-1}$ represent the known constant matrices reflecting the structural information of parameter perturbation, the positive scalars α_a and α_b are chosen by the designer. $\Delta_{ai} = \Delta J(I + J_0^{-1}\Delta J)^{-1}J_0^{-1}\omega^{\times}(J_0 + \Delta J) - \omega^{\times}\Delta J$ and $\Delta_b = \Delta J(I + J_0^{-1}\Delta J)^{-1}$ represent the unknown matrix of parameter perturbation. Clearly, there exist positive scalars δ_{ai} and δ_b such that $\|\Delta_{ai}\| \le \delta_{ai}$ and $\|\Delta_b\| \le \delta_b$.

Remark 3. Here, the measurement matrix C_i is identity, which indicates that the measurement frame coincides with the satellite body frame O_B. However, C_i is not necessarily identity, that is, the measurement frame does not coincide with O_B. When the pairs (A_i, C_i) are observable, the following fuzzy adaptive observer can be applied. It should be pointed out that C_i is obviously a non-singular matrix, and the value of C_i does not affect the subsequent derivation of Theorem 1 and 2. The measurement matrix C_i is used to solve the premise variable $z(t)$ from the measurement output $y(t)$ when C_i is not an identity matrix. In this paper, for brevity, C_i is selected as an identity matrix, which is a common choice and also adopted by literature [1, 42, 43]. Thus, we retain C_i so that the method proposed can be applied to general systems.

Remark 4. The actuator faults existing in the dynamic equation can be propagated to the kinematic equation through the closed-loop satellite attitude control system. However, based on observer design theory, we here only need to use the dynamic equation to diagnose and estimate the actuator fault. Thus, the premise variables of T-S fuzzy model are only variables attitude angular velocity $\omega(t)$, which greatly reduces the number of model rules and the complexity of the T-S fuzzy system.

The defuzzification process of the model (10) can be represented as

$$\begin{aligned} \dot{x}(t) &= \sum_{i=1}^{r} h_i(z(t))\left\{(A_i + \Delta A_i)x(t) + (B + \Delta B)\left(u(t) + f(t)\right) + B_d d(t)\right\} \\ y(t) &= Cx(t) \end{aligned} \tag{11}$$

where $\chi(t) = [\chi_1(t) \quad \chi_2(t) \quad \chi_3(t)]$, $h_i(\chi(t)) = \frac{\prod_{j=1}^{p} M_j^i(\chi_j(t))}{\sum_{i=1}^{r}\prod_{j=1}^{p} M_j^i(\chi_j(t))}$ with the properties that $0 \le M_j^i(\chi_j(t)) \le 1$ and $\sum_{i=1}^{r} h_i(\chi(t)) = 1$.

Based on the above model, some reasonable assumptions are introduced to support the main results.

Assumption 1. The external disturbance $d(t)$ is bounded with $\|d(t)\| \le \kappa_d$, where the upper bound $\kappa_d \ge 0$ exists but is unknown.

Assumption 2. The actuator fault $f(t)$ is bounded with $\|f(t)\| \le \kappa_f$, where $\kappa_f \ge 0$ is unknown.

Assumption 3. The angular velocity $\omega(t)$ own bounded first-order derivative.

Assumptions 1 and 2 are some general constraints and have been widely used in literature [4, 13, 28, 44], which are reasonable in practical applications owing to physical limitations. Assumption 3 is natural and reasonable because signals $\omega(t)$ and $\dot{\omega}(t)$ are energy-bounded in practical systems, which is often considered in studies [3, 13, 14, 28, 29, 45].

Before the main results of this study, some necessary lemmas are introduced as follows.

Lemma 1. *[46]: Given symmetric positive definite matrix P, then*

$$\begin{bmatrix} \xi \\ \pi \end{bmatrix}^T \begin{bmatrix} \langle PA \rangle_S & PB \\ * & 0 \end{bmatrix} \begin{bmatrix} \xi \\ \pi \end{bmatrix} < 0 \tag{12}$$

holds for any $\xi \ne 0$ and π satisfying $\pi^T\pi \le \xi^T C^T C \xi$ if and only if there exists a scalar $\sigma \ge 0$, such that

$$\begin{bmatrix} \langle PA \rangle_S + \sigma C^T C & PB \\ * & -\sigma I \end{bmatrix} < 0 \tag{13}$$

Lemma 2. *[19]: The eigenvalues of a given matrix $\mathcal{A}$ belong to the circular region $O(\phi, \varepsilon)$ with centre $\phi + j0$ and radius ε if and only if there exists a symmetric positive definite matrix Q such that the following condition holds*

$$\begin{bmatrix} -Q & Q(\mathcal{A} - \phi I) \\ * & -\varepsilon^2 Q \end{bmatrix} < 0 \tag{14}$$

Lemma 3. *[46]: Let P, Q and $H = H^T$ be given matrices of appropriate dimensions, N_P and N_Q be the right orthogonal complements of P and Q, respectively. Then there exists a matrix X such that*

$$H + P^T X^T Q + Q^T X P < 0 \tag{15}$$

if and only if

$$N_P^T H N_P < 0, N_Q^T H N_Q < 0 \tag{16}$$

3 | MAIN RESULTS

This section mainly introduces the design of the proposed FAFEO for satellite attitude system, including the sufficient existence condition, feasibility proof and LMI algorithm. An H_∞ method is utilized to attenuate the influence of model uncertainties on actuator fault estimation. Moreover, a further relaxed stability condition is represented in terms of LMI.

3.1 | Fuzzy adaptive observer design with AP

The following error vectors are defined as

$$\begin{aligned} e(t) &= x(t) - \hat{x}(t) \\ r(t) &= y(t) - \hat{y}(t) \\ e_f(t) &= f(t) - \hat{f}(t) \end{aligned} \tag{17}$$

where $\hat{x}(t)$ and $\hat{y}(t)$ are the estimated state and output vectors, respectively. $\hat{f}(t)$ is the online estimation of fault $f(t)$. $e(t)$, $r(t)$ and $e_f(t)$ denote the state error, residual error and fault estimate error, respectively.

For the studied system (11), the FAFEO with AP is constructed as

$$\begin{aligned} \dot{\hat{x}}(t) &= \sum_{i=1}^{r} h_i(\chi(t)) \left\{ A_i\hat{x}(t) + Bu(t) + B\hat{f}(t) + K_i(y(t) - \hat{y}(t)) \right\} \\ \hat{y}(t) &= C\hat{x}(t) \\ \dot{\hat{f}}(t) &= \sum_{i=1}^{r} h_i(\chi(t)) \left\{ F_{1i}(y(t) - \hat{y}(t)) + \vartheta F_2(\dot{y}(t) - \dot{\hat{y}}(t)) \right\} \end{aligned} \tag{18}$$

where K_i and F_{1i} are the unknown gain matrices with appropriate dimensions to be designed. The gain matrix F_2 and adjustable scalar ϑ are chosen by the designer.

Subtracting system (18) from (11), the dynamic error equation is obtained by

$$\begin{aligned} \dot{e}(t) &= \sum_{i=1}^{r} h_i(\chi(t)) \left\{ (A_i - K_iC)\, e(t) + Be_f(t) + \Delta A_i x(t) + \Delta Bu(t) + \Delta Bf(t) \right\} \\ r(t) &= Ce(t) \\ \dot{e}_f(t) &= \sum_{i=1}^{r} h_i(\chi(t)) \left\{ \dot{f}(t) - F_{1i}Ce(t) - \vartheta F_2 C\dot{e}(t) \right\} \end{aligned} \tag{19}$$

By defining a new variable $\bar{e}^T(t) = [e^T(t) \; e_f^T(t)]$, the fuzzy system (19) can be rewritten as

$$\begin{aligned} \bar{M}\dot{\bar{e}}(t) &= \sum_{i=1}^{r} h_i(\chi(t)) \left\{ \left(\bar{A}_i - \bar{K}_i C\right) \bar{e}(t) + \bar{B}_d \bar{d}(t) \right\} \\ e_f(t) &= \bar{I}_{ef}\bar{e}(t) \end{aligned} \tag{20}$$

where $\bar{M} = \begin{bmatrix} I & 0 \\ \vartheta F_2 C & I \end{bmatrix}$, $\bar{A}_i = \begin{bmatrix} A_i & B \\ 0 & 0 \end{bmatrix}$, $\bar{K}_i = \begin{bmatrix} K_i \\ F_{1i} \end{bmatrix}$, $\bar{C} = [C\ 0]$, $\bar{I}_{ef} = [0_3\ I_3]$, $\bar{B}_d = \begin{bmatrix} \Delta A_i & \Delta B & \Delta B & B_d & 0 \\ 0 & 0 & 0 & 0 & I \end{bmatrix}$, $\bar{d}^T(t) = [x^T(t)\ u^T(t)\ f^T(t)\ d^T(t)\ \dot{f}^T(t)]$

It is obvious that $\bar{M}$ is non-singular irrespective of the term $\vartheta F_2 C$. Thus, the augmented dynamic error equation can be derived that

$$\begin{aligned} \dot{\bar{e}}(t) &= \sum_{i=1}^{r} h_i(\chi(t)) \left\{ \bar{M}^{-1} \left(\bar{A}_i - \bar{K}_i C \right) \bar{e}(t) + \bar{M}^{-1} \bar{B}_d \bar{d}(t) \right\} \\ e_f(t) &= \bar{I}_{ef} \bar{e}(t) \end{aligned} \tag{21}$$

Performing Laplace transformation on (21), the fault estimation error can be derived from

$$\begin{aligned} e_f(s) &= G_{ef\bar{d}}(s) \bar{d}(s) \\ G_{ef\bar{d}}(s) &= \sum_{i=1}^{r} h_i(\chi(t)) \left\{ \bar{I}_{ef} \left[sI - \bar{M}^{-1} (\bar{A}_i - \bar{K}_i \bar{C}) \right]^{-1} \bar{M}^{-1} \bar{B}_d \right\} \end{aligned} \tag{22}$$

where $G_{ef\bar{d}}(s)$, a multivariable function of $\{K_i, F_{1i}, F_2, \vartheta\}$, is the transfer function from $\bar{d}(t)$ to $e_f(t)$. Obviously, $e_f(t)$ is not only related to $\dot{f}(t)$ and $d(t)$, but also related to $x(t)$, $u(t)$ and $f(t)$ caused by parameter perturbation. In order to attenuate the effect of above model uncertainties, an H_∞ method is introduced into the design of FAFEO with AP.

Remark 5. From (19), the online fault estimator can be derived as

$$\hat{f}(t) = \sum_{i=1}^{r} h_i(\chi(t)) \left\{ F_{1i} \int_{t_0}^{t} Ce(\tau) d\tau + \vartheta F_2 Ce(t) - \vartheta F_2 Ce(t_0) \right\}$$

where t_0 denotes a certain moment before the fault occurrence. It is obvious that the presented fault estimator $\hat{f}(t)$ is a PI function of $e(t)$, where only the current measurement output are required. Compared with some observer methods [8, 10], the added adjustable proportional term provide additional design freedom to the fault estimator, and can clearly enhance the rapidity and accuracy of actuator fault estimation, which is verified in Section 4.

3.2 | Observer-based fault estimation design

Theorem 1. *For systems (11) and (18), let an H_∞ performance index $\gamma_1 > 0$, an auxiliary index $\gamma_2 > 0$, and a circular pole constraint region $O(\phi, \varepsilon)$ for $\bar{M}^{-1}(\bar{A}_i - \bar{K}_i C)$ be given. For prescribed scalars ϑ, δ, and matrix F_2, if there exist matrices $\bar{Y}_i$, $P > 0$ satisfying*

$$\begin{bmatrix} \left\langle \bar{M}^T P \bar{A}_i - \bar{M}^T \bar{Y}_i C \right\rangle_S & 0 & \bar{M}^T P \hat{B}_d & \bar{M}^T P \hat{H} & I_{ef}^T \\ * & \delta \hat{N}^T \hat{N} - \gamma_1^2 I & 0 & 0 & 0 \\ * & * & -\gamma_2^2 I & 0 & 0 \\ * & * & * & -I & 0 \\ * & * & * & * & -I \end{bmatrix} < 0 \tag{23}$$

$$\begin{bmatrix} -P & -\phi P \bar{M}^T + P \bar{A}_i - \bar{Y}_i C \\ * & -\varepsilon^2 \bar{M}^T P \bar{M} \end{bmatrix} < 0 \tag{24}$$

where $\delta \geq \max_i \|\hat{R}_i^T \hat{R}_i\|$, $\hat{B}_d = \begin{bmatrix} B_d & 0 \\ 0 & I \end{bmatrix}$, $\hat{H} = \begin{bmatrix} D_a & D_b \\ 0 & 0 \end{bmatrix}$, $\hat{R}_i = \begin{bmatrix} \Delta_{ai} & 0 \\ 0 & \Delta_b \end{bmatrix}$, $\hat{N} = \begin{bmatrix} E_a & 0 & 0 \\ 0 & E_b & E_b \end{bmatrix}$, $\gamma_2 \leq \gamma_1$ then the augmented system (21) is asymptotically stable and satisfies $\|G_{ef\bar{d}}(s)\|_\infty < \gamma_1$. The gain matrices of the fuzzy adaptive observer are computed by $\bar{K}_i = P^{-1} \bar{Y}_i$.

Proof. Since $\bar{M}$ is non-singular, for an symmetric positive definite matrix P, the matrix $\bar{M}^T P \bar{M}$ is also symmetric positive definite. Define the Lyapunov candidate as

$$V(t) = \bar{e}^T(t) \bar{M}^T P \bar{M} \bar{e}(t) \tag{25}$$

Obviously, $V(t)$ is positive definite.

Firstly, the stability of the augmented system (21) with $\bar{d}(t) = 0$ is proved. Substituting Equation (21), the time derivative of (25) is

$$\begin{aligned} \dot{V}(t) &= \dot{\bar{e}}^T(t) \bar{M}^T P \bar{M} \bar{e}(t) + \bar{e}^T(t) \bar{M}^T P \bar{M} \dot{\bar{e}}(t) \\ &= \sum_{i=1}^{r} h_i(\chi(t)) \bar{e}^T(t) \left(\bar{A}_i - \bar{K}_i C \right)^T \bar{M}^{-T} \bar{M}^T P \bar{M} \bar{e}(t) \\ &\quad + \sum_{i=1}^{r} h_i(\chi(t)) \bar{e}^T(t) \bar{M}^T P \bar{M} \bar{M}^{-1} \left(\bar{A}_i - \bar{K}_i C \right) \bar{e}(t) \\ &= \sum_{i=1}^{r} h_i(\chi(t)) \left\{ \bar{e}^T(t) \left\langle \bar{M}^T P \left(\bar{A}_i - \bar{K}_i C \right) \right\rangle_S \bar{e}(t) \right\} \end{aligned} \tag{26}$$

From (26), it can be readily found that $\dot{V}(t) < 0$ is equivalent to

$$\left\langle \bar{M}^T P \left(\bar{A}_i - \bar{K}_i C \right) \right\rangle_S < 0 \tag{27}$$

Therefore, based on Lyapunov stability theorem, the augmented system (21) is asymptotically stable when the inequality (27) is satisfied.

Then, when $\bar{d}(t) \neq 0$, it is proved that (21) has H_∞ performance index [19, 44]

$$\left\| G_{ef\bar{d}}(s) \right\|_\infty = \sup_\omega \bar{\sigma}(G_{ef\bar{d}}(j\omega)) < \gamma_1 \tag{28}$$

Defining new matrices $\hat{B}_d$, $\hat{H}$, $\hat{R}_i$, $\hat{N}$, and new variables $\hat{u}^T(t) = [x^T(t)\ u^T(t)\ f^T(t)]$ and $\hat{d}^T(t) = [d^T(t)\ \dot{f}^T(t)]$, we could obtain $\bar{d}^T(t) = [\hat{u}^T(t)\ \hat{d}^T(t)]$ and $\bar{B}_d = [\hat{H}\hat{R}_i\hat{N}\ \hat{B}_d]$. Then, the time derivative of (25) with $\bar{d}(t) \neq 0$ is

$$\begin{aligned}
\dot{V}(t) &= \dot{\bar{e}}^T(t)\bar{M}^T P\bar{M}\bar{e}(t) + \bar{e}^T(t)\bar{M}^T P\bar{M}\dot{\bar{e}}(t) \\
&= \sum_{i=1}^{r} h_i(z(t)) \left\{ \bar{e}^T(t) \left\langle \bar{M}^T P \left(\bar{\mathcal{A}}_i - \bar{K}_i C \right) \right\rangle_S \bar{e}(t) + 2\bar{e}^T(t)\bar{M}^T P\bar{B}_d\bar{d}(t) \right\} \\
&= \sum_{i=1}^{r} h_i(z(t)) \bar{e}^T(t) \left\langle \bar{M}^T P \left(\bar{\mathcal{A}}_i - \bar{K}_i C \right) \right\rangle_S \bar{e}(t) \\
&\quad + \sum_{i=1}^{r} h_i(z(t)) 2\bar{e}^T(t)\bar{M}^T P\hat{H}\hat{R}_i\hat{N}\hat{u}(t) + \sum_{i=1}^{r} h_i(z(t)) 2\bar{e}^T(t)\bar{M}^T P\hat{B}_d\hat{d}(t) \\
&= \sum_{i=1}^{r} h_i(z(t)) \left\{ \bar{e}^T(t) \left\langle M^T P \left(\bar{\mathcal{A}}_i - \bar{K}_i C \right) \right\rangle_S \bar{e}(t) + 2\bar{e}^T(t)\bar{M}^T P\hat{B}_d\hat{d}(t) \right\} \\
&\quad + \sum_{i=1}^{r} h_i(z(t)) \left\{ \bar{e}^T(t)\bar{M}^T P\hat{H}\hat{H}P\bar{M}\bar{e}(t) + \hat{u}^T(t)\hat{N}^T\hat{R}_i^T\hat{R}_i\hat{N}\hat{u}(t) \right\} \\
&\quad - \sum_{i=1}^{r} h_i(z(t)) \left(\bar{e}^T(t)\bar{M}^T P\hat{H} - \hat{u}^T(t)\hat{N}^T\hat{R}_i^T \right) \\
&\quad \times \left(\bar{e}^T(t)\bar{M}^T P\hat{H} - \hat{u}^T(t)\hat{N}^T\hat{R}_i^T \right)^T
\end{aligned} \tag{29}$$

Furthermore, due to the bounded parameter uncertainties $\Delta\mathcal{A}_i$ and ΔB, the positive scalar δ exists and satisfies

$$\delta \geq \max_i \left\| \hat{R}_i^T\hat{R}_i \right\| \tag{30}$$

Then,

$$\begin{aligned}
\dot{V}(t) &\leq \sum_{i=1}^{r} h_i(z(t)) \left\{ \bar{e}^T(t) \left\langle M^T P \left(\bar{\mathcal{A}}_i - \bar{K}_i C \right) \right\rangle_S \bar{e}(t) + 2\bar{e}^T(t)\bar{M}^T P\hat{B}_d\hat{d}(t) \right\} \\
&+ \sum_{i=1}^{r} h_i(z(t)) \left\{ \bar{e}^T(t)\bar{M}^T P\hat{H}\hat{H}P\bar{M}\bar{e}(t) + \hat{u}^T(t)\delta\hat{N}^T\hat{N}\hat{u}(t) \right\} \\
&- \sum_{i=1}^{r} h_i(z(t)) \left(\bar{e}^T(t)\bar{M}^T P\hat{H} - \hat{u}^T(t)\hat{N}^T\hat{R}_i^T \right) \left(\bar{e}^T(t)\bar{M}^T P\hat{H} - \hat{u}^T(t)\hat{N}^T\hat{R}_i^T \right)^T
\end{aligned} \tag{31}$$

For any $t > 0$, let us define

$$J = \int_{t_0}^{t} \left(e_f^T(\tau)e_f(\tau) - \gamma_1^2\bar{d}^T(\tau)\bar{d}(\tau) \right) d\tau \tag{32}$$

By introducing a new index γ_2 with the constraint $\gamma_2 \leq \gamma_1$, we have

$$\begin{aligned}
J &= \int_{t_0}^{t} \left(e_f^T(\tau)e_f(\tau) - \gamma_1^2\bar{d}^T(\tau)\bar{d}(\tau) \right) d\tau \\
&= \int_{t_0}^{t} \left(e_f^T(\tau)e_f(\tau) - \gamma_1^2\hat{u}^T(\tau)\hat{u}(\tau) - \gamma_2^2\hat{d}^T(\tau)\hat{d}(\tau) - (\gamma_1^2 - \gamma_2^2)\hat{d}^T(\tau)\hat{d}(\tau) \right) d\tau \\
&\leq \int_{t_0}^{t} \left(e_f^T(\tau)e_f(\tau) - \gamma_1^2\hat{u}^T(\tau)\hat{u}(\tau) - \gamma_2^2\hat{d}^T(\tau)\hat{d}(\tau) \right) d\tau
\end{aligned} \tag{33}$$

Under zero initial condition $V(t_0) = 0$ [43, 47], we get

$$\begin{aligned}
J &\leq \int_{t_0}^{t} \left(e_f^T(\tau)e_f(\tau) - \gamma_1^2\hat{u}^T(\tau)\hat{u}(\tau) - \gamma_2^2\hat{d}^T(\tau)\hat{d}(\tau) + \dot{V}(\tau) - \dot{V}(\tau) \right) d\tau \\
&= \sum_{i=1}^{r} h_i(z(t)) \int_{t_0}^{t} \left\{ \bar{e}^T(\tau)\bar{I}_{ef}^T\bar{I}_{ef}\bar{e}(\tau) - \gamma_1^2\hat{u}^T(\tau)\hat{u}(\tau) - \gamma_2^2\hat{d}^T(t)\hat{d}(t) \right. \\
&+ \bar{e}^T(\tau) \left\langle M^T P \left(\bar{\mathcal{A}}_i - \bar{K}_i C \right) \right\rangle_S \bar{e}(\tau) + 2\bar{e}^T(\tau)\bar{M}^T P\hat{B}_d\hat{d}(\tau) \\
&+ \bar{e}^T(\tau)\bar{M}^T P\hat{H}\hat{H}P\bar{M}\bar{e}(\tau) + \hat{u}^T(\tau)\delta\hat{N}^T\hat{N}\hat{u}(\tau) \\
&\left. - \left(\bar{e}^T(\tau)\bar{M}^T P\hat{H} - \hat{u}^T(\tau)\hat{N}^T\hat{R}_i^T \right) \left(\bar{e}^T(\tau)\bar{M}^T P\hat{H} - \hat{u}^T(\tau)\hat{N}^T\hat{R}_i^T \right)^T \right\} d\tau \\
&+ V(t_0) - V(t)
\end{aligned}$$

Then

$$J \leq \sum_{i=1}^{r} h_i(z(t)) \int_{t_0}^{t} \left\{ \xi^T(\tau)\Xi\xi(\tau) - \Xi_0 \right\} d\tau - V(t) \tag{34}$$

where

$$\xi(\tau) = \begin{bmatrix} \bar{e}(\tau) \\ \hat{u}(\tau) \\ \hat{d}(\tau) \end{bmatrix},$$

$$\Xi = \begin{bmatrix} \langle \bar{M}^T P(\bar{\mathcal{A}}_i - \bar{K}_i C) \rangle_S + \bar{I}_{ef}^T\bar{I}_{ef} + \bar{M}^T P\hat{H}\hat{H}P\bar{M} & 0 & \bar{M}^T P\hat{B}_d \\ * & \delta\hat{N}^T\hat{N} - \gamma_1^2 I & 0 \\ * & * & -\gamma_2^2 I \end{bmatrix},$$

$$\Xi_0 = (\bar{e}^T(\tau)\bar{M}^T P\hat{H} - \hat{u}^T(\tau)\hat{N}^T\hat{R}_i^T)(\bar{e}^T(\tau)\bar{M}^T P\hat{H} - \hat{u}^T(\tau)\hat{N}^T\hat{R}_i^T)^T$$

Hence, the index $J < 0$, which is equivalent to $\|G_{ef\bar{d}}(s)\|_\infty < \gamma_1$, can be satisfied by

$$\Xi < 0 \tag{35}$$

According to Schur complement [10], (35) is converted to

$$\begin{bmatrix} \left\langle \bar{M}^T P \left(\bar{\mathcal{A}}_i - \bar{K}_i C \right) \right\rangle_S + \bar{I}_{ef}^T\bar{I}_{ef} & 0 & \bar{M}^T P\hat{B}_d & \bar{M}^T P\hat{H} \\ * & \delta\hat{N}^T\hat{N} - \gamma_1^2 I & 0 & 0 \\ * & * & -\gamma_2^2 I & 0 \\ * & * & * & -I \end{bmatrix} < 0 \tag{36}$$

Obviously (36) holds while implying that inequality (27) also holds. Finally, we have the condition (23) results from (36) by defining $\bar{Y}_i = P\bar{K}_i$ and Schur complement.

Now, the convergence of $e_f(t)$ is proved.

According to Lemma 1 and assuming that $\sigma = 1$, for (35), when

$$e_f^T(t)e_f(t) = \bar{e}^T(t)\bar{I}_{ef}^T\bar{I}_{ef}\bar{e}(t) \geq \gamma_1^2\hat{u}^T(t)\hat{u}(t) + \gamma_2^2\hat{d}^T(t)\hat{d}(t) \tag{37}$$

it can guarantee that

$$\dot{V}(t) = \sum_{i=1}^{r} h_i(z)\begin{bmatrix}\bar{e}(t)\\ \hat{u}(t)\\ \hat{d}(t)\end{bmatrix}^T\begin{bmatrix}\left\langle \bar{M}^T P\left(\bar{A}_i - \bar{K}_i C\right)\right\rangle_S + \bar{M}^T P\hat{H}\hat{H}P\bar{M} & 0 & \bar{M}^T P\hat{B}_d\\ * & \delta\hat{N}^T\hat{N} & 0\\ * & * & 0\end{bmatrix}\begin{bmatrix}\bar{e}(t)\\ \hat{u}(t)\\ \hat{d}(t)\end{bmatrix} < 0 \tag{38}$$

and there is $T > 0$, for any $t > t_0 + T$ such that

$$\left\|e_f(t)\right\|_2 \leq \gamma_1\left\|\hat{u}(t)\right\|_2 + \gamma_2\left\|\hat{d}(t)\right\|_2 \tag{39}$$

which means the dynamic error system (21) is asymptotically stable and fault estimate error $e_f(t)$ is ultimately uniformly bounded.

By Lemma 2, there is a symmetric positive definite matrix $\bar{M}^T P\bar{M}$ such that

$$\mathrm{E} = \begin{bmatrix}-\bar{M}^T P\bar{M} & -\phi\bar{M}^T P\bar{M} + \bar{M}^T P(\bar{A}_i - \bar{K}_i\bar{C})\\ * & -\varepsilon^2\bar{M}^T P\bar{M}\end{bmatrix} < 0 \tag{40}$$

from which it follows that the eigenvalues of $\bar{M}^{-1}(\bar{A}_i - \bar{K}_i C)$ belong to the given circular region $\mathrm{O}(\phi, \varepsilon)$. Then we can get (24) by $\bar{Y}_i = P\bar{K}_i$ and the transformation of MEM^T with $\mathrm{M} = diag(\bar{M}^{-1}, I)$. This completes the proof. □

Remark 6. Without the auxiliary index γ_2, the (35) becomes

$$\Xi = \begin{bmatrix}\left\langle \bar{M}^T P\left(\bar{A}_i - \bar{K}_i C\right)\right\rangle_S + \bar{I}_{ef}^T\bar{I}_{ef} + \bar{M}^T P\hat{H}\hat{H}P\bar{M} & 0 & \bar{M}^T P\hat{B}_d\\ * & \delta\hat{N}^T\hat{N} - \gamma_1^2 I & 0\\ * & * & -\gamma_1^2 I\end{bmatrix} < 0 \tag{41}$$

For (41), when $e_f^T(t)e_f(t) = \bar{e}^T(t)\bar{I}_{ef}^T\bar{I}_{ef}\bar{e}(t) \geq \gamma_1^2\bar{d}^T(t)\bar{d}(t)$, it could guarantee that constraint (38) holds. Therefore, there is $T > 0$, for any $t > t_0 + T$ such that $\|e_f(t)\|_2 \leq \gamma_1\|\hat{u}(t)\|_2 + \gamma_1\|\hat{d}(t)\|_2$. With the comparison, the condition (37) and (39) are able to guarantee Theorem 1 could be relaxed.

Remark 7. In Theorem 1, the pole assignment condition with a circular constraint region is considered. The transient performance of the dynamic error system (21) can be adjusted by selecting different regions $\mathrm{O}(\phi, \varepsilon)$, where the centre $\phi + j0$ is related to the convergence rate of the system and the appropriate radius ε could ensure that the system (21) will not have a large overshoot.

Remark 8. In Theorem 1, adjustable parameter ϑ is added to improve the fault estimation performance by increasing the design flexible of the proposed method. For the proposed proportional-integral fuzzy fault estimator (19), it is difficult to solve design parameters owing to the nonlinear term $\bar{M}^T P$ existing in LMIs. We could select an appropriate full row rank matrix F_2 and a suitable parameter ϑ by testing more to enhance the fault estimation performance, which also avoid the nonlinear term $\bar{M}^T P$ existing in LMIs while the computing burden and algorithmic complexity are not too much increased. Meanwhile, reviewing the existing approaches [48, 49], H_∞ design and regional pole placement are effective methods in dealing with disturbance and tuning the transient response, respectively. We combine H_∞ design with regional pole placement to assist the fuzzy adaptive observer and improve the fault estimation performance. However, there is more conservatism due to a common Lyapunov matrix P involved in multiple LMIs. The following Theorem 2 will give design parameters with less conservatism, see Remarks 9 and 10.

3.3 | Fault estimation design with less conservatism

In Theorem 1, a multi-objective design method is given to calculate above design parameters. However, a common Lyapunov matrix $P(Q = P)$ is involved for two constraints (23) and (24), which has been considered in [19, 20]. In this subsection, based on the elimination method, different Lyapunov matrices P and Q can exist independently of each other in the two constraints, which results in less conservatism.

Theorem 2. *For systems (11) and (18), let an H_∞ performance index $\gamma_1 > 0$, an auxiliary index $\gamma_2 > 0$, and a circular pole constraint region $O(\phi, \varepsilon)$ for $\bar{M}^{-1}(\bar{A}_i - \bar{K}_i C)$ be given. For prescribed scalars ϑ, δ, and matrix F_2, if there exist symmetric positive definite matrices P, Q satisfying*

$$\begin{bmatrix} \Theta_{11i} & 0 & \Theta_{13} & \Theta_{14} & \Theta_{15} \\ * & \Theta_{22} & 0 & 0 & 0 \\ * & * & -\gamma_2^2 I & 0 & 0 \\ * & * & * & -I & 0 \\ * & * & * & * & -I \end{bmatrix} < 0 \tag{42}$$

$$\begin{bmatrix} -Q & -\phi Q\bar{M}N_{\bar{C}2} + Q\bar{A}_i N_{\bar{C}2} \\ * & -\varepsilon^2 N_{\bar{C}2}^T \bar{M}^T Q \bar{M} N_{\bar{C}2} \end{bmatrix} < 0 \tag{43}$$

where $\Theta_{11i} = N_{\bar{C}1}^T \bar{M}^T P \bar{A}_i N_{\bar{C}1} + N_{\bar{C}1}^T \bar{A}_i^T P \bar{M} N_{\bar{C}1}$, $\Theta_{22} = \delta \hat{N}^T \hat{N} - \gamma_1^2 I$ $\Theta_{13} = N_{\bar{C}1}^T \bar{M}^T P \hat{B}_d$, $\Theta_{14} = N_{\bar{C}1}^T \bar{M}^T P \hat{H}$, $\Theta_{15} = N_{\bar{C}1}^T \bar{I}_{ef}^T$ $\delta \geq \max_i \|\hat{R}_i^T \hat{R}_i\|$, $\hat{B}_d = \begin{bmatrix} B_d & 0 \\ 0 & I \end{bmatrix}$, $\hat{H} = \begin{bmatrix} D_a & D_b \\ 0 & 0 \end{bmatrix}$, $\hat{R}_i = \begin{bmatrix} \Delta_{ai} & 0 \\ 0 & \Delta_b \end{bmatrix}$, $\hat{N} = \begin{bmatrix} E_a & 0 & 0 \\ 0 & E_b & E_b \end{bmatrix}$, $\gamma_2 \leq \gamma_1$ $N_{\bar{C}1}$ and $N_{\bar{C}2}$ are the right orthogonal complements of $\bar{C}$. Note that $N_{\bar{C}1}$ and $N_{\bar{C}2}$ could be different. Then, the augmented system (21) is asymptotically stable and satisfies $\|G_{\bar{e}f\bar{d}}(s)\|_\infty < \gamma_1$, and the observer gain matrix $\bar{K}_i$ is given by

$$\begin{bmatrix} \langle \bar{M}^T P(\bar{A}_i - \bar{K}_i C) \rangle_S & 0 & \bar{M}^T P \hat{B}_d & \bar{M}^T P \hat{H} & \bar{I}_{ef}^T \\ * & \delta \hat{N}^T \hat{N} - \gamma_1^2 I & 0 & 0 & 0 \\ * & * & -\gamma_2^2 I & 0 & 0 \\ * & * & * & -I & 0 \\ * & * & * & * & -I \end{bmatrix} < 0 \tag{44}$$

$$\begin{bmatrix} -Q & -\phi Q\bar{M}^T + Q(\bar{A}_i - \bar{K}_i C) \\ * & -\varepsilon^2 \bar{M}^T Q \bar{M} \end{bmatrix} < 0 \tag{45}$$

Proof. Based on Theorem 1, here only requires to prove that (44) and (45) are equivalent to (42) and (43), respectively. Note that (23) and (24) is one special case of (44) and (45) with the assumption $P = Q$.

Firstly, define

$$H_{P_i} = \begin{bmatrix} \langle \bar{M}^T P \bar{A}_i \rangle_S & 0 & \bar{M}^T P \hat{B}_d & \bar{M}^T P \hat{H} & \bar{I}_{ef}^T \\ * & \delta \hat{N}^T \hat{N} - \gamma_1^2 I & 0 & 0 & 0 \\ * & * & -\gamma_2^2 I & 0 & 0 \\ * & * & * & -I & 0 \\ * & * & * & * & -I \end{bmatrix}$$

$$H_{Q_i} = \begin{bmatrix} -Q & -\phi Q\bar{M} + Q\bar{A}_i \\ * & -\varepsilon^2 \bar{M}^T Q \bar{M} \end{bmatrix} \tag{46}$$

Then, the formulas (23) and (24) are converted to

$$\begin{aligned} H_{P_i} + U_P^T \bar{K}_i W_1 + W_1^T \bar{K}_i^T U_P < 0 \\ H_{Q_i} + U_Q^T \bar{K}_i W_2 + W_2^T \bar{K}_i^T U_Q < 0 \end{aligned} \tag{47}$$

where $U_P = [-P\bar{M}\ 0\ 0\ 0\ 0]$, $U_Q = [-Q\ 0]$ $W_1 = [\bar{C}\ 0\ 0\ 0\ 0]$, $W_2 = [0\ \bar{C}]$

By Lemma 3, formula (47) is feasible if and only if

$$N_{U_P}^T H_{P_i} N_{U_P} < 0,\ N_{U_Q}^T H_{Q_i} N_{U_Q} < 0 \tag{48}$$

$$N_{W1}^T H_{P_i} N_{W1} < 0,\ N_{W2}^T H_{Q_i} N_{W2} < 0 \tag{49}$$

where N_{U_P}, N_{U_Q}, N_{W1} and N_{W2} are the right orthogonal complements of U_P, U_Q, W_1 and W_2, respectively. To convert (48) to an LMI, the linearization is given as follows.

Define $S_P = diag(P\bar{M}\ I\ I\ I\ I)$, $S_Q = diag(Q\ I)$. Then

$$U_1 = U_P S_P^{-1} = \begin{bmatrix} -I & 0 & 0 & 0 & 0 \end{bmatrix},\ U_2 = U_Q S_Q^{-1} = \begin{bmatrix} -I & 0 \end{bmatrix} \tag{50}$$

$$T_{P_i} = (S_P^{-1})^T H_{P_i} (S_P^{-1})$$

$$= \begin{bmatrix} \langle \bar{A}_i \bar{M}^{-1} P^{-1} \rangle_S & 0 & \hat{B}_d & \hat{H} & P^{-1}\bar{M}^{-T}\bar{I}_{ef}^T \\ * & \delta \hat{N}^T \hat{N} - \gamma_1^2 I & 0 & 0 & 0 \\ * & * & -\gamma_2^2 I & 0 & 0 \\ * & * & * & -I & 0 \\ * & * & * & * & -I \end{bmatrix}$$

$$T_{Q_i} = (S_Q^{-1})^T H_{Q_i} (S_Q^{-1})$$

$$= \begin{bmatrix} -Q^{-1} & -\phi\bar{M} + \bar{A}_i \\ * & -\varepsilon^2 \bar{M}^T Q \bar{M} \end{bmatrix} \tag{51}$$

Hence(48) is equivalent to

$$N_{U1}^T T_{P_i} N_{U1} < 0,\ N_{U2}^T T_{Q_i} N_{U2} < 0 \tag{52}$$

where N_{U1} and N_{U2} are the right orthogonal complements of U_1 and U_2, respectively.

Finally, we can obtain

$$N_{U1}^T T_{P_i} N_{U1} = \begin{bmatrix} \Theta_{22} & 0 & 0 & 0 \\ * & -\gamma_2^2 I & 0 & 0 \\ * & * & -I & 0 \\ * & * & * & -\varepsilon I \end{bmatrix} < 0 \tag{53}$$

$$N_{U2}^T T_{Q_i} N_{U2} = -\varepsilon^2 \bar{M}^T Q \bar{M} < 0 \tag{54}$$

$$N_{W1}^T H_{P_i} N_{W1} = \left[\begin{array}{c|ccc} \Theta_{11i} & 0 & \Theta_{13} & \Theta_{14} \quad \Theta_{15} \\ \hline * & \multicolumn{3}{c}{N_{U1}^T T_{P_i} N_{U1}} \end{array}\right] < 0 \tag{55}$$

$$N_{W2}^T H_{Q_i} N_{W2} = \left[\begin{array}{c|c} -Q & -\phi Q \bar{M} N_{\bar{C}2} + Q \bar{A}_i N_{\bar{C}2} \\ \hline * & -\varepsilon^2 N_{\bar{C}2}^T \bar{M}^T Q \bar{M} N_{\bar{C}2} \end{array}\right] < 0 \tag{56}$$

where $N_{U1} = \begin{bmatrix} 0 \\ diag(I,I,I,I) \end{bmatrix}$, $N_{U2} = \begin{bmatrix} 0 \\ I \end{bmatrix}$, $N_{W1} = diag(N_{\bar{C}1}, I, I, I, I)$, $N_{W2} = diag(I, N_{\bar{C}2})$

Obviously, inequality (54) holds. Invoking Schur complement on (55) leads to that (53)–(56) are equivalent to (42), (43).

Clearly, inequalities (44) and (45) become LMIs containing only the matrix variables $\bar{K}_i$, when formulas (42) and (43) are both established. Moreover, the existence of variables obtained in (42) and (43) has ensured that (44) and (45) are feasible.

This completes the proof. □

Remark 9. In (44), (45), the terms of $\bar{Y}_{1i} = P\bar{K}_i$ and $\bar{Y}_{2i} = Q\bar{K}_i$ lead to the coupling between variables P and Q due to the common variable $\bar{K}_i$. Obviously, there is a strict implicit constraint $P^{-1}\bar{Y}_{1i} = Q^{-1}\bar{Y}_{2i}$, which makes it more difficult to calculate design parameters. In Theorem 1, we adopt a simple but strong assumption $Q = P$, which reduces the difficulty of optimization problem, but increases the conservatism. In Theorem 2, under the elimination technique, we achieve the decoupling of P and $\bar{K}_i$ by separating these variables from the term $P\bar{K}_i$, and the same is applied to $Q\bar{K}_i$. Therefore, the linearization of constraints and the independence of Lyapunov matrices P and Q can be realized simultaneously.

Remark 10. For any set of possible solutions in inequalities (23) and (24), gain matrices K_i and F_{1i} are determined by parameters $\{P, Q, \gamma_1, \gamma_2\}$. Thus, the algorithm conservatism comparison between Theorem 1 and 2 can be obtained by the parameter analysis of $\{P, Q, \gamma_1, \gamma_2\}$ in constraints (23), (24) and (42), (43). Firstly, the parameter analysis between (23) and (42) is given. By Lemma 3, there is N_{U_P}, for any feasible solutions in (23), such that $N_{U_P}^T(H_{P_i} + U_P^T \bar{K}_i W_1 + W_1^T \bar{K}_i^T U_P)N_{U_P} = N_{U_P}^T H_{P_i} N_{U_P} < 0$, which shows that all feasible solutions of (23) must also meet (42). Similarly, all feasible solutions of (24) must also satisfy (43), thus is omitted here for brevity. It can be seen that, Theorem 1 is a special case of Theorem 2 under the precondition $Q = P$. Compared with Theorem 1, in the same context, Theorem 2 can improve the flexibility of observer design and provide design conditions with less conservatism. Moreover, the Theorem 3 in [19] gives another method to solve this by using the slack-variable technique, which different Lyapunov matrices can be involved for the two constraints. Comparison and analysis between above four methods will be shown in the following section clearly.

The procedure of obtaining the design parameters of the proposed method is summarized as follows:

Step 1: Selecting an appropriate full row rank matrix F_2.

Step 2: Selecting the parameter interval $(\vartheta_{\min}, \vartheta_{\max})$ and the step length α_k to obtain a set of working points $(\vartheta_{\min}, \vartheta_{\min} + \alpha_k, \ldots, \vartheta_{\min} + (n-1)\alpha_k, \vartheta_{\max})$, $n = (\vartheta_{\max} - \vartheta_{\min})/\alpha_k$, while too large parameters may lead to no feasible solution.

Step 3: Solving the Theorem 1 or Theorem 2 to attain the design parameters.

Step 4: Based on numerical simulation, the quantitative performance indexes of fault estimation are given, including $IAE = \int_0^T |e_f(t)|dt$ (integrated absolute error) and $ITAE = \int_0^T t|e_f(t)|dt$ (integrated time absolute error).

a. If the index distribution is not obvious or there is no complete distribution trend, increase the parameter range $(\vartheta_{\min}, \vartheta_{\max})$, and return to Step 2.
b. If the index distribution possesses a complete and obvious distribution trend, the calculation is end. The lowest work point of the index distribution curve is the relatively optimal parameter to be found.

4 | NUMERICAL SIMULATION

In this section, simulation results on a rigid satellite are provided to show the effectiveness and advantage of the proposed method. The numerical simulation including two parts: (a) Simulation results based on Theorem 1; (b) Simulation results based on Theorem 2. And two observers proposed in [10, 19] are considered as comparisons. To quantitatively characterize the fault estimation performance and show the benefits of the proposed method, two metrics are introduced to evaluate the transient performance and the steady state performance of the fault tracking response, including $IAE = \int_0^T |e_f(t)|dt$ (integrated absolute error) and $ITAE = \int_0^T t|e_f(t)|dt$ (integrated time absolute error) [50].

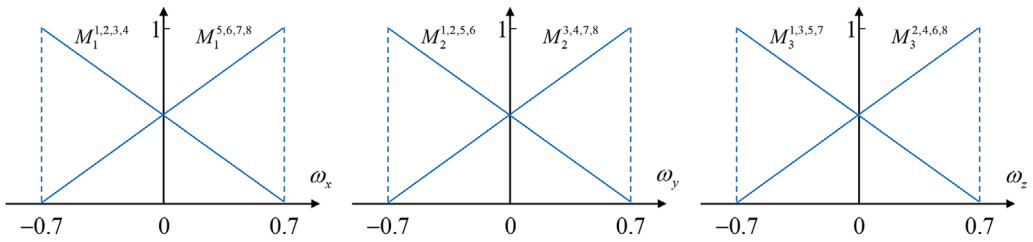

FIGURE 1 Membership functions of the rule premise

The nominal inertia matrix and the external disturbances of satellite attitude system are given as follows [1, 43]:

$$J_0 = \begin{bmatrix} 18 & 0.1 & 0.2 \\ 0.1 & 21 & 1 \\ 0.2 & 1 & 23 \end{bmatrix} \text{kg} \cdot \text{m}^2$$

$$d(t) = \begin{bmatrix} 1.5 \times 10^{-5}(3\cos(\omega_0 t) + 1) \\ 1.5 \times 10^{-5}(3\cos(\omega_0 t) + 1.5\sin(\omega_0 t)) \\ 1.5 \times 10^{-5}(3\sin(\omega_0 t) + 1) \end{bmatrix} \text{N} \cdot \text{m}$$

with $\omega_0 = 0.0011\text{rad/s}$

The parameter perturbation of inertia matrix is selected as

$$\Delta J = \begin{bmatrix} 0.2 & -0.02 & 0.04 \\ -0.02 & 0.3 & 0.1 \\ 0.02 & 0.05 & 0.3 \end{bmatrix} e^{-0.02t} \text{kg} \cdot \text{m}^2$$

We consider three scenarios of actuator faults: fault-free (healthy), intermittent fault, and fast time varying fault. Here are three channels defined as

$$f_1(t) = 0\text{N} \cdot \text{m}$$

$$f_2(t) = \begin{cases} 0.1\text{N} \cdot \text{m} & 2\text{ s} \le t \\ 0\text{N} \cdot \text{m} & \text{others} \end{cases}$$

$$f_3(t) = \begin{cases} 0\text{N} \cdot \text{m} & 0\text{ s} \le t \le 1\text{ s} \\ 0.1\sin(2t)\text{N} \cdot \text{m} & 1\text{ s} < t \end{cases}$$

The proposed method is assessed on a usual feedback control loop, that is, PID control with the amplitude of driving torque limited to $0.5\text{N} \cdot \text{m}$ due to actuator physical constraints. Besides, $\beta = 5$, PID controller gains are designed by $k_p = 0.8$, $k_i = 0$, $k_d = 4$. The initial states are chosen by $q_v^T(0) = [0.3\ 0.2\ -0.4]$, $\omega(0) = 0_{3\times1}$. Assume that the initial states are the desired. The observer initial states are given by $\hat{\omega}(0) = 0_{3\times1}$.

The operating regions of premise variables are defined as $\omega_j(t) \in [-0.7\ 0.7]\text{rad/s}$, $j = 1, 2, 3$. Choosing eight operating points, the membership functions of fuzzy sets $M_j^i (i = 1, 2, \ldots, 8, j = 1, 2, 3)$ are illustrated in Figure 1 [38]. The T-S fuzzy model of the rigid satellite is expressed as follows.

Model rule 1: IF $\omega(t)$ is $[0.7\ 0.7\ 0.7]$, THEN

$$\dot{x}(t) = (A_1 + \Delta A_1)x(t) + (B + \Delta B)\big(u(t) + f(t)\big) + B_d d(t)$$

Model rule 2: IF $\omega(t)$ is $[0.7\ 0.7\ -0.7]$, THEN

$$\dot{x}(t) = (A_2 + \Delta A_2)x(t) + (B + \Delta B)\big(u(t) + f(t)\big) + B_d d(t)$$

Model rule 3: IF $\omega(t)$ is $[0.7\ -0.7\ 0.7]$, THEN

$$\dot{x}(t) = (A_3 + \Delta A_3)x(t) + (B + \Delta B)\big(u(t) + f(t)\big) + B_d d(t)$$

Model rule 4: IF $\omega(t)$ is $[0.7\ -0.7\ -0.7]$, THEN

$$\dot{x}(t) = (A_4 + \Delta A_4)x(t) + (B + \Delta B)\big(u(t) + f(t)\big) + B_d d(t)$$

Model rule 5: IF $\omega(t)$ is $[-0.7\ 0.7\ 0.7]$, THEN

$$\dot{x}(t) = (A_5 + \Delta A_5)x(t) + (B + \Delta B)\big(u(t) + f(t)\big) + B_d d(t)$$

Model rule 6: IF $\omega(t)$ is $[-0.7\ 0.7\ -0.7]$, THEN

$$\dot{x}(t) = (A_6 + \Delta A_6)x(t) + (B + \Delta B)\big(u(t) + f(t)\big) + B_d d(t)$$

Model rule 7: IF $\omega(t)$ is $[-0.7\ -0.7\ 0.7]$, THEN

$$\dot{x}(t) = (A_7 + \Delta A_7)x(t) + (B + \Delta B)\big(u(t) + f(t)\big) + B_d d(t)$$

Model rule 8: IF $\omega(t)$ is $[-0.7\ -0.7\ -0.7]$, THEN

$$\dot{x}(t) = (A_8 + \Delta A_8)x(t) + (B + \Delta B)\big(u(t) + f(t)\big) + B_d d(t)$$

4.1 | Simulation results based on Theorem 1

First, according to (30), $\delta = 10 \ge \max_i \|\hat{R}_i^T \hat{R}_i\| = 7.4873$, where $\alpha_a = 0.1$, $\alpha_b = 0.1$. Invoking the Schur complement on (23) leads to the condition $\hat{N}^T \hat{R}^T \hat{R} \hat{N} - \gamma_1^2 I < 0$, $\|\delta \hat{N}^T \hat{N}\|_2 = 6.1792$, we could select $\gamma_1^2 = 6.18$. The full row

TABLE 1 Comparison of performance index under three different ϑ

ϑ	γ_2	$e_{f2}(t)$		$e_{f3}(t)$	
0 (Ref. [10])	0.2179	IAE2 = 1.2690	ITAE2 = 2.6250	IAE3 = 2.502	ITAE3 = 4.9110
−10	0.2176	IAE2 = 2.0280	ITAE2 = 4.1650	IAE3 = 3.3430	ITAE3 = 6.6380
20	0.2607	IAE2 = 0.2337	ITAE2 = 0.4887	IAE3 = 0.7564	ITAE3 = 0.9756

rank matrix F_2 is selected as

$$F_2=\begin{bmatrix}100 & 0 & 0\\ * & 100 & 0\\ * & * & 100\end{bmatrix}$$

A fault estimation method based on adaptive observer is considered to draw comparison. The adaptive fault estimator in Ref. [10] can be designed as

$$\dot{\hat{f}}(t) = F_1\left(y(t)-\hat{y}(t)\right) \tag{57}$$

where F_1 is gain matrix. Note that the proposed Theorem 1 will degenerate into the method in [10] when $\vartheta = 0$, that is, the adaptive fault estimator (57) is a special case of the proposed (18).

We set regional pole constraints as $O(-50, 50)$, the feasibility radius of LMIs in Theorem 1 as 1×10^7, and $\gamma_2^2 \le 0.1$, which are conducive to avoid the singularity of observer gain matrix $\bar{K}_i$ and improve the numerical stability. By Theorem 1 and trying different parameter ϑ, we can conveniently get the performance index. With the selection of $T = 6$s, comparative results of performance index are illustrated in Table 1 and Figure 2. Where ITAE2 and IAE2 represent the fault estimation performance index of the intermittent fault $f_2(t)$. ITAE3 and IAE3 represent the fault estimation performance index of the fast time varying fault $f_3(t)$. Instead of H_∞ performance index γ_2, under the same simulation conditions, the index ITAE has higher precision and better sensitivity to parameter and can provide more reliable decisions.

By Theorem 1 with $\vartheta = 0$, we can obtain

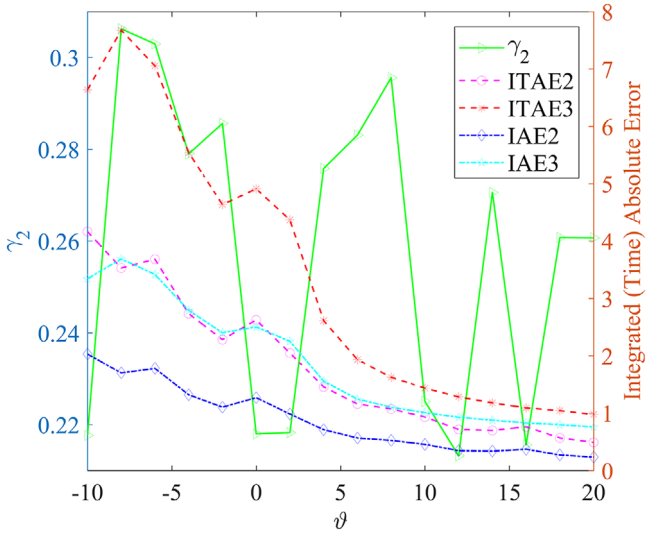

FIGURE 2 Change of performance index with different ϑ

$$F_{11}=\begin{bmatrix}1.1594\times 10^4 & 25.1371 & 51.7888\\ 26.4627 & 1.2399\times 10^4 & 239.1533\\ 50.3789 & 240.7114 & 1.2879\times 10^4\end{bmatrix}$$

$$K_1=\begin{bmatrix}75.5130 & 0.7804 & -0.8511\\ -0.6151 & 75.5773 & 0.7878\\ 0.5699 & -0.6135 & 75.5243\end{bmatrix}$$

$$P=\begin{bmatrix}2.2500\times 10^4 & 27.9400 & 55.2431 & -60.1723 & -0.0451 & -0.0899\\ * & 2.3370\times 10^4 & 260.1674 & -0.0451 & -61.5412 & -0.4418\\ * & * & 2.3891\times 10^4 & -0.0899 & -0.4418 & -62.4249\\ * & * & * & 0.3733 & -0.0004 & -0.0007\\ * & * & * & * & 0.3613 & -0.0031\\ * & * & * & * & * & 0.3552\end{bmatrix}$$

$$F_{12}=\begin{bmatrix}1.1594\times10^{4} & 26.5739 & 51.8515\\ 25.1522 & 1.2399\times10^{4} & 239.1412\\ 50.3611 & 240.7150 & 1.2879\times10^{4}\end{bmatrix}$$

$$K_{2}=\begin{bmatrix}75.4992 & -0.8423 & -0.9284\\ 0.5785 & 75.5910 & 0.8014\\ 0.5179 & -0.5999 & 75.5244\end{bmatrix}$$

$$F_{13}=\begin{bmatrix}1.1594\times10^{4} & 25.0746 & 50.2268\\ 26.4806 & 1.2399\times10^{4} & 239.1516\\ 51.7250 & 240.7176 & 1.2879\times10^{4}\end{bmatrix}$$

$$K_{3}=\begin{bmatrix}75.5404 & 0.8578 & 0.9263\\ -0.5630 & 75.5772 & 0.7806\\ -0.5195 & -0.6202 & 75.4970\end{bmatrix}$$

$$F_{14}=\begin{bmatrix}1.1594\times10^{4} & 26.5114 & 50.2895\\ 25.1701 & 1.2399\times10^{4} & 239.1393\\ 51.7073 & 240.7210 & 1.2879\times10^{4}\end{bmatrix}$$

$$K_{4}=\begin{bmatrix}75.5265 & -0.7649 & 0.8490\\ 0.6306 & 75.5910 & 0.7942\\ -0.5715 & -0.6066 & 75.4971\end{bmatrix}$$

$$K_{6}=\begin{bmatrix}75.4992 & -0.8558 & -0.9213\\ 0.5650 & 75.4639 & -0.7268\\ 0.5245 & 0.6740 & 75.6515\end{bmatrix}$$

$$F_{17}=\begin{bmatrix}1.1594\times10^{4} & 25.0710 & 50.2286\\ 26.4928 & 1.2399\times10^{4} & 240.7671\\ 51.7190 & 239.1932 & 1.2879\times10^{4}\end{bmatrix}$$

$$K_{7}=\begin{bmatrix}75.5404 & 0.8442 & 0.9334\\ -0.5766 & 75.4501 & -0.7476\\ -0.5128 & 0.6537 & 75.6241\end{bmatrix}$$

$$F_{18}=\begin{bmatrix}1.1594\times10^{4} & 26.5079 & 50.2912\\ 25.1823 & 1.2399\times10^{4} & 240.7547\\ 51.7011 & 239.1966 & 1.2879\times10^{4}\end{bmatrix}$$

$$K_{8}=\begin{bmatrix}75.5265 & -0.7785 & 0.8561\\ 0.6170 & 75.4638 & -0.7340\\ -0.5649 & 0.6672 & 75.6242\end{bmatrix}$$

By Theorem 1 with $\vartheta = 20$, we can obtain

$$P=\begin{bmatrix}1.6952\times10^{5} & 6.5170\times10^{3} & 1.1938\times10^{4} & -100.7491 & -2.9259 & -5.3127\\ * & 4.1929\times10^{5} & 3.2665\times10^{4} & -2.9259 & -215.2222 & -13.2652\\ * & * & 4.8418\times10^{5} & -5.3127 & -13.2660 & -241.5355\\ * & * & * & 0.0689 & 0.0013 & 0.0023\\ * & * & * & * & 0.1201 & 0.0054\\ * & * & * & * & * & 0.1308\end{bmatrix}$$

$$F_{15}=\begin{bmatrix}1.1594\times10^{4} & 25.1337 & 51.7907\\ 26.4750 & 1.2399\times10^{4} & 240.7688\\ 50.3729 & 239.1871 & 1.2879\times10^{4}\end{bmatrix}$$

$$K_{5}=\begin{bmatrix}75.5130 & 0.7669 & -0.8439\\ -0.6286 & 75.4501 & -0.7404\\ 0.5766 & 0.6604 & 75.6514\end{bmatrix}$$

$$F_{16}=\begin{bmatrix}1.1594\times10^{4} & 26.5705 & 51.8532\\ 25.1645 & 1.2399\times10^{4} & 240.7566\\ 50.3549 & 239.1907 & 1.2879\times10^{4}\end{bmatrix}$$

$$F_{11}=\begin{bmatrix}7.1818\times10^{4} & 1.5878\times10^{3} & 696.2723\\ -330.1929 & 9.6923\times10^{4} & 9.5434\times10^{3}\\ 2.3525\times10^{3} & 7.0505\times10^{3} & 1.1149\times10^{5}\end{bmatrix}$$

$$K_{1}=\begin{bmatrix}24.4294 & 1.6181 & 0.0975\\ -0.3982 & 46.7642 & 5.5889\\ 1.9133 & 3.6659 & 54.7600\end{bmatrix}$$

$$F_{12}=\begin{bmatrix}7.1820\times10^{4} & -123.4131 & 585.7826\\ 1.5777\times10^{3} & 9.6952\times10^{4} & 9.5840\times10^{3}\\ 1.9422\times10^{3} & 7.0514\times10^{3} & 1.1147\times10^{5}\end{bmatrix}$$

$$K_2=\begin{bmatrix}24.4151 & -0.4500 & -0.0106\\ 1.3663 & 46.7926 & 5.6105\\ 1.6018 & 3.6936 & 54.7501\end{bmatrix}$$

$$F_{13}=\begin{bmatrix}7.1876\times10^{4} & 1.7577\times10^{3} & 2.6158\times10^{3}\\ 102.6588 & 9.6927\times10^{4} & 9.5414\times10^{3}\\ 1.2279\times10^{3} & 7.0214\times10^{3} & 1.1144\times10^{5}\end{bmatrix}$$

$$K_3=\begin{bmatrix}24.4856 & 1.7399 & 2.3680\\ -0.0801 & 46.7664 & 5.5739\\ 0.7546 & 3.6517 & 54.7053\end{bmatrix}$$

$$F_{14}=\begin{bmatrix}7.1844\times10^{4} & 51.4975 & 2.5079\times10^{3}\\ 2.0143\times10^{3} & 9.6969\times10^{4} & 9.6208\times10^{3}\\ 817.7941 & 7.0509\times10^{3} & 1.1142\times10^{5}\end{bmatrix}$$

$$K_4=\begin{bmatrix}24.4566 & -0.3263 & 2.2611\\ 1.6859 & 46.8003 & 5.6139\\ 0.4432 & 3.6940 & 54.6972\end{bmatrix}$$

$$F_{15}=\begin{bmatrix}7.1816\times10^{4} & 1.5933\times10^{3} & 694.3891\\ -391.0359 & 9.5880\times10^{4} & 5.9687\times10^{3}\\ 2.3623\times10^{3} & 8.5254\times10^{3} & 1.1254\times10^{5}\end{bmatrix}$$

$$K_5=\begin{bmatrix}24.4283 & 1.5859 & 0.1071\\ -0.4310 & 46.1036 & 3.0068\\ 1.9190 & 4.9216 & 55.4224\end{bmatrix}$$

$$F_{16}=\begin{bmatrix}7.1821\times10^{4} & -85.4250 & 551.8898\\ 1.5494\times10^{3} & 9.5902\times10^{4} & 6.0043\times10^{3}\\ 1.9603\times10^{3} & 8.5365\times10^{3} & 1.1252\times10^{5}\end{bmatrix}$$

$$K_6=\begin{bmatrix}24.4154 & -0.4704 & -0.0051\\ 1.3461 & 46.1285 & 3.0251\\ 1.6126 & 4.9537 & 55.4148\end{bmatrix}$$

$$F_{17}=\begin{bmatrix}7.1875\times10^{4} & 1.6657\times10^{3} & 2.6463\times10^{3}\\ -14.6095 & 9.5884\times10^{4} & 5.9643\times10^{3}\\ 1.2711\times10^{3} & 8.5096\times10^{3} & 1.1248\times10^{5}\end{bmatrix}$$

$$K_7=\begin{bmatrix}24.4853 & 1.6797 & 2.3896\\ -0.1332 & 46.1054 & 2.9898\\ 0.7735 & 4.9129 & 55.3682\end{bmatrix}$$

$$F_{18}=\begin{bmatrix}7.1875\times10^{4} & -9.0070 & 2.5053\times10^{3}\\ 1.9303\times10^{3} & 9.5921\times10^{4} & 6.0545\times10^{3}\\ 869.8663 & 8.5333\times10^{3} & 1.1247\times10^{5}\end{bmatrix}$$

$$K_8=\begin{bmatrix}24.4570 & -0.3753 & 2.2778\\ 1.6459 & 46.1377 & 3.0349\\ 0.4674 & 4.9521 & 55.3591\end{bmatrix}$$

Figure 3 and 4 show the comparison of simulation results under the intermittent fault and fast time varying fault respectively, which is consistent with the performance index ITAE. Obviously, the proposed observer can estimate both the system states and two different types of actuator faults simultaneously, and all estimation errors asymptotically converge to a small bounded interval. In particular, the system state estimation errors $e(t)$ will show the fluctuation with fault characteristics as the actuator fault occurs, such as the large initial error caused by abrupt changing characteristics and the tracking lagging error caused by time varying characteristics. It can be seen clearly that, a better design is implemented by finding appreciate parameter ϑ. Compared with the observer in [10], the proposed method could have lower fault estimation errors and higher estimation accuracy. The proposed method enhances the tracking response speed of fault estimation under the premise of added adjustable proportional terms, and effectively suppresses the tracking lead or lag caused by fault changing, especially for fast time varying faults. The results above verify the effectiveness of the proposed AP-based method.

Moreover, the external disturbances and actuator faults with different amplitude are used to analyse the performance of the method proposed. Note that these conditions are only used here.

Case 1. Small external disturbances [42].

$$d(t)=\begin{bmatrix}-1.5+2\times\cos(0.06t)-0.5\cos(0.2t)\\ 2+1.5\times\sin(0.06t)-1\cos(0.2t)\\ -1.5+2\times\sin(0.06t)-1.5\sin(0.2t)\end{bmatrix}10^{-4}\mathrm{N}\cdot\mathrm{m}$$

Case 2. Large external disturbances.

$$d(t)=\begin{bmatrix}-1.5+2\times\cos(0.06t)-0.5\cos(0.2t)\\ 2+1.5\times\sin(0.06t)-1\cos(0.2t)\\ -1.5+2\times\sin(0.06t)-1.5\sin(0.2t)\end{bmatrix}10^{-3}\mathrm{N}\cdot\mathrm{m}$$

The following time-varying faults are adopted.

$$f_1(t)=f_2(t)=0\mathrm{N}\cdot\mathrm{m}$$

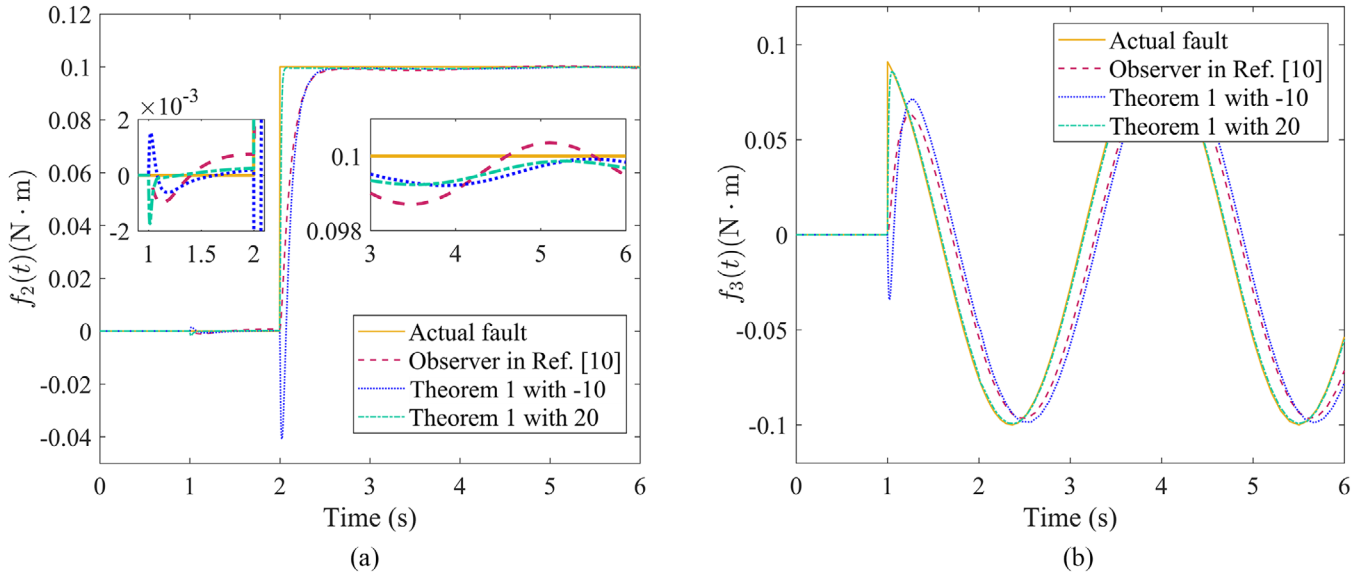

FIGURE 3 Comparison of fault estimation: (a) intermittent fault f_2(b) fast time varying fault f_3

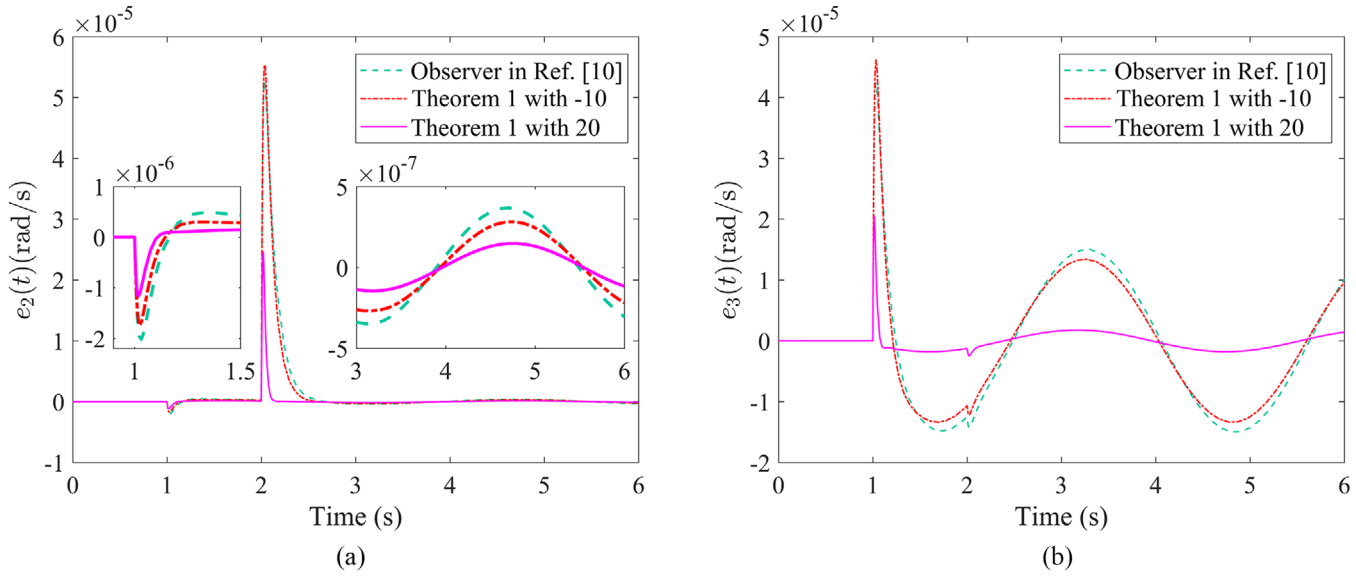

FIGURE 4 Comparison of system state estimation errors: (a) e_2(b) e_3

$$f_3(t) = \begin{cases} 0\text{N} \cdot \text{m0s} \le t \le 1\text{s} \\ k_{am} \sin(2t)\text{N} \cdot \text{m1s} < t \end{cases}$$

where $k_{am} \in \{0.1, 0.2, 0.4\}$ (input saturation $u_{\max} = 0.5$).

Figure 5 and 6 show the comparison of different amplitude faults under small and large external disturbances, respectively. Where the same scale means that $e_{f3}(t)/(10k_{am})$. (1) Under the same external disturbances, the fault estimation error will increase with the increase of fault amplitude, where the increase is generally proportional. (2) Under the same faults, the fault estimation error will increase with the increase of external disturbances amplitude, while the increase is not obvious for heavy fault. It is worth mentioning that, under the large external disturbances, it is more difficult to estimate weak faults (see Figure 6b).

4.2 | Simulation results based on Theorem 2

In this subsection, the benefit of the proposed method is further demonstrated by the meticulous comparison with different methods and more general satellite operating conditions. The gain matrix F_2, regional pole constraints, and simulation

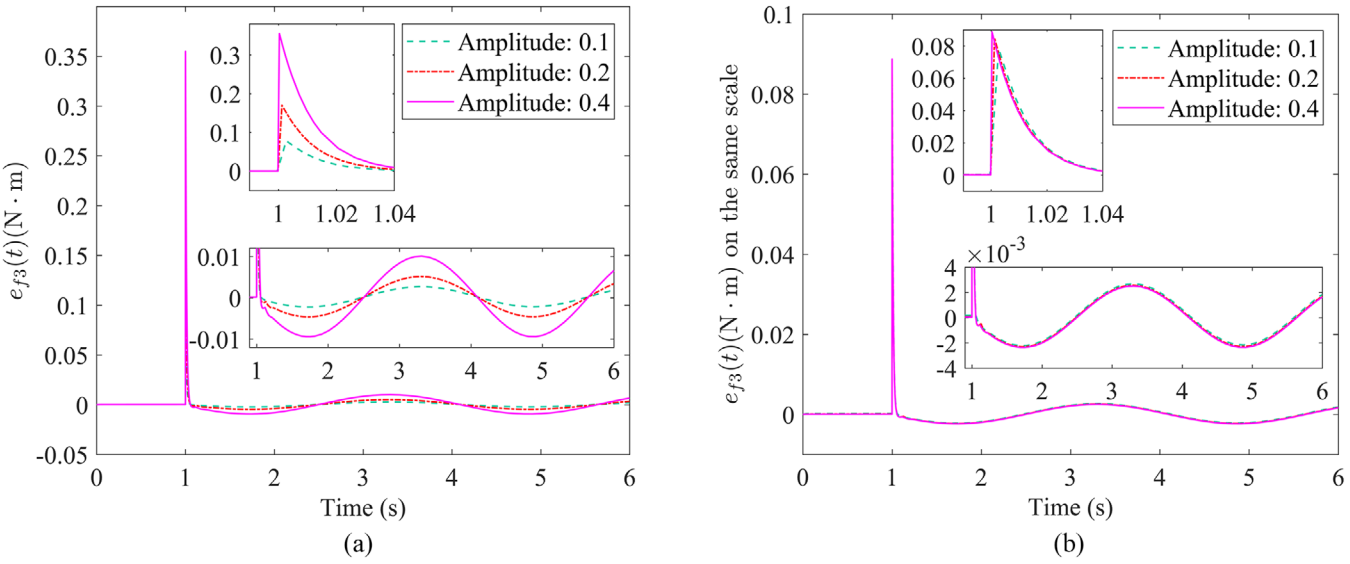

FIGURE 5 Comparison of fault estimation error (small external disturbances): (a) e_{f3}(b) e_{f3} on the same scale

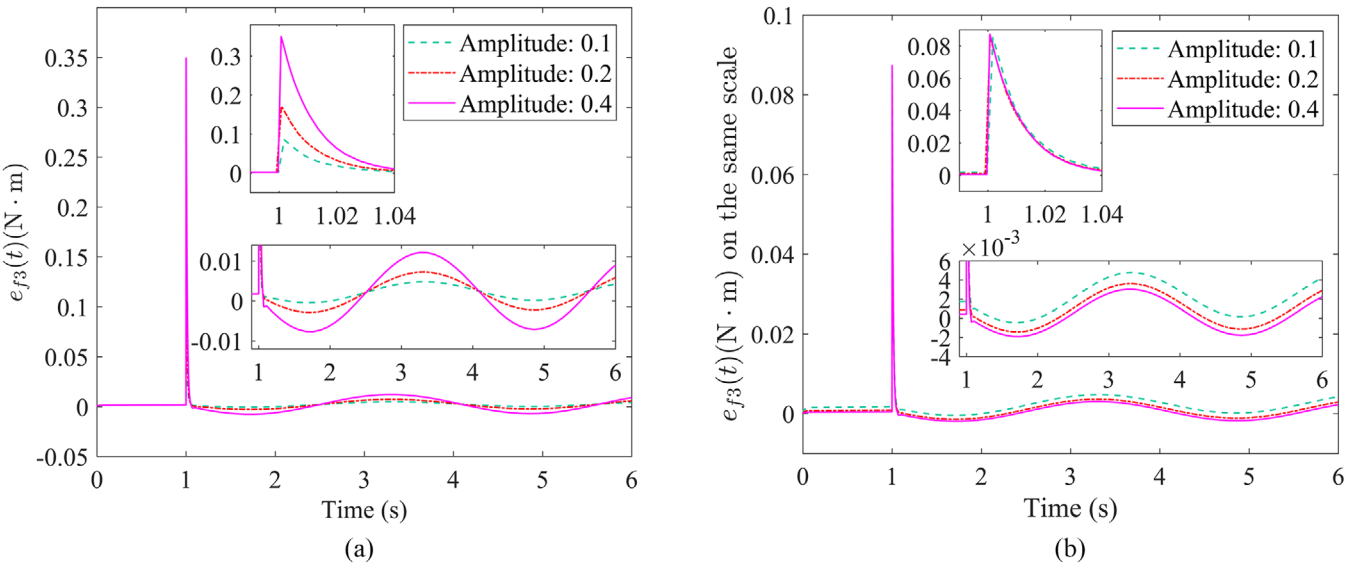

FIGURE 6 Comparison of fault estimation error (large external disturbances): (a) e_{f3}(b) e_{f3} on the same scale

conditions are the same to those in Theorem 1. Similarly, we can get the performance indexes, which are illustrated in Figure 7. Figure 8 shows the feasible areas in the varying regions ($-40 \leq \vartheta \leq 40$) according to Theorem 3 in Ref. [19], Theorem 1 without the auxiliary index γ_2, Theorem 1, and Theorem 2, respectively. It is shown that, from the perspective of feasible area, Theorem 3 in Ref. [19] has the most conservative results and Theorem 2 gives the most relaxed results.

A more general case is considered. The system initial states are chosen by $q_v^T(0) = [0.3\ 0.2\ -0.4]$, $\omega^T(0) = [0.1\ 0.2\ -0.1]$rad/s. The desired attitude and angle velocity are given by $q_{dv}^T(0) = [-0.1\ 0.3\ 0.1]$ and $\omega_d(0) = 0_{3\times1}$. Considering unpredictable deviations caused by time delays, observer initial states are given by $\hat{\omega}(0) = 0.8\omega(0)$.

We consider the new three scenarios of actuator faults: fault-free (healthy), intermittent fault, and fast time varying fault. Here are three channels defined as

$$f_1(t) = 0\text{N} \cdot \text{m}$$

$$f_2(t) = \begin{cases} 0.1\text{N} \cdot \text{m} 10\text{ s} \leq t \leq 20\text{ s} \\ (0.14 - 0.002t)\text{ N} \cdot \text{m} 20\text{ s} < t \\ 0\text{N} \cdot \text{mothers} \end{cases}$$

$$f_3(t) = \begin{cases} 0\text{N} \cdot \text{m} 0\text{s} \leq t \leq 8\text{s} \\ 0.1\sin(2t)\text{N} \cdot \text{m} 8\text{s} < t \end{cases}$$

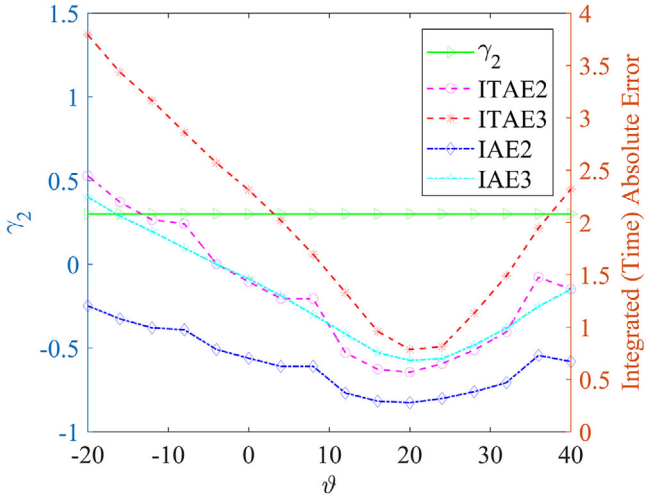

FIGURE 7 Change of performance index with different ϑ

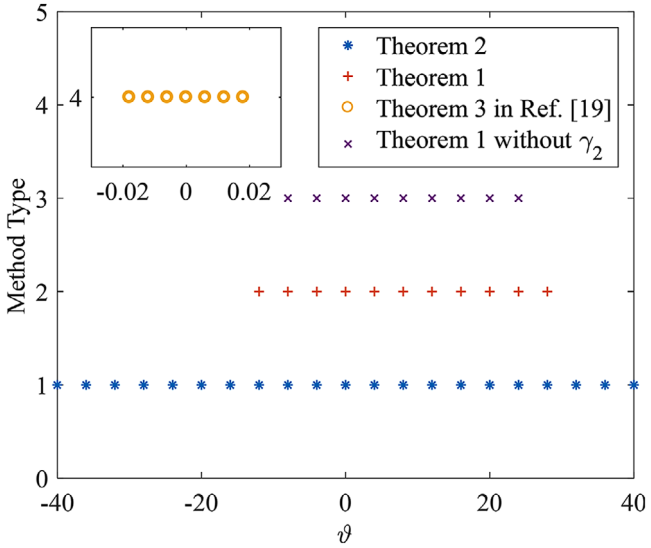

FIGURE 8 Feasible area for the stabilization of four methods

By Theorem 2 with $\vartheta = 20$, we can obtain, $\gamma_2 = 0.2487$

$$P = \begin{bmatrix} 2.9709 \times 10^5 & 116.7380 & 236.0223 & -86.6855 & -0.4730 & -0.9454 \\ * & 2.9968 \times 10^5 & 1.2427 \times 10^3 & -0.4730 & -100.9009 & -4.7130 \\ * & * & 3.0159 \times 10^5 & -0.9454 & -4.7130 & -110.3254 \\ * & * & * & 0.5025 & 1.3898 \times 10^{-4} & 2.8085 \times 10^{-4} \\ * & * & * & * & 0.5066 & 0.0015 \\ * & * & * & * & * & 0.5059 \end{bmatrix}$$

$$Q = \begin{bmatrix} 3.5998 \times 10^5 & 2.6645 \times 10^3 & 5.2460 \times 10^3 & -276.1707 & -0.6391 & -1.2176 \\ * & 4.3648 \times 10^5 & 2.4931 \times 10^4 & -0.6551 & -294.3821 & -5.1255 \\ * & * & 4.8208 \times 10^5 & -1.2688 & -5.2229 & -302.5944 \\ * & * & * & 0.3434 & -3.8219 \times 10^{-4} & -7.6594 \times 10^{-4} \\ * & * & * & * & 0.3303 & -0.0038 \\ * & * & * & * & * & 0.3217 \end{bmatrix}$$

$$F_{11} = \begin{bmatrix} 1.7048 \times 10^4 & -1.4395 & 2.5521 \\ -2.7684 & 1.6717 \times 10^4 & 125.5132 \\ -1.4906 & 119.8547 & 1.6940 \times 10^4 \end{bmatrix}$$

$$K_1 = \begin{bmatrix} -10.8260 & 1.0359 & -0.3516 \\ -0.3768 & -3.4961 & 3.2899 \\ 1.0568 & 1.8484 & 1.3489 \end{bmatrix}$$

$$F_{12} = \begin{bmatrix} 1.7048 \times 10^4 & -1.4395 & 2.5521 \\ -2.7684 & 1.6717 \times 10^4 & 125.5132 \\ -1.4906 & 119.8547 & 1.6940 \times 10^4 \end{bmatrix}$$

$$K_2 = \begin{bmatrix} -10.8399 & -0.5977 & -0.4295 \\ 0.8258 & -3.4823 & 3.3036 \\ 1.0047 & 1.8620 & 1.3490 \end{bmatrix}$$

$$F_{13}=\begin{bmatrix}1.7048\times10^{4} & -1.4395 & 2.5521\\ -2.7684 & 1.6717\times10^{4} & 125.5132\\ -1.4906 & 119.8547 & 1.6940\times10^{4}\end{bmatrix}$$

$$K_3=\begin{bmatrix}-10.7985 & 1.1138 & 1.4376\\ -0.3246 & -3.4961 & 3.2826\\ -0.0413 & 1.8416 & 1.3215\end{bmatrix}$$

$$F_{14}=\begin{bmatrix}1.7048\times10^{4} & -1.4395 & 2.5521\\ -2.7684 & 1.6717\times10^{4} & 125.5132\\ -1.4906 & 119.8547 & 1.6940\times10^{4}\end{bmatrix}$$

$$K_4=\begin{bmatrix}-10.8124 & -0.5198 & 1.3597\\ 0.8780 & -3.4823 & 3.2963\\ -0.0935 & 1.8552 & 1.3216\end{bmatrix}$$

$$F_{15}=\begin{bmatrix}1.7048\times10^{4} & -1.4395 & 2.5521\\ -2.7684 & 1.6717\times10^{4} & 125.5132\\ -1.4906 & 119.8547 & 1.6940\times10^{4}\end{bmatrix}$$

$$K_5=\begin{bmatrix}-10.8260 & 1.0223 & -0.3445\\ -0.3904 & -3.6238 & 1.7504\\ 1.0635 & 3.1323 & 1.4767\end{bmatrix}$$

$$F_{16}=\begin{bmatrix}1.7048\times10^{4} & -1.4395 & 2.5521\\ -2.7684 & 1.6717\times10^{4} & 125.5132\\ -1.4906 & 119.8547 & 1.6940\times10^{4}\end{bmatrix}$$

$$K_6=\begin{bmatrix}-10.8399 & -0.6112 & -0.4224\\ 0.8121 & -3.6100 & 1.7641\\ 1.0114 & 3.1459 & 1.4768\end{bmatrix}$$

$$F_{17}=\begin{bmatrix}1.7048\times10^{4} & -1.4395 & 2.5521\\ -2.7684 & 1.6717\times10^{4} & 125.5132\\ -1.4906 & 119.8547 & 1.6940\times10^{4}\end{bmatrix}$$

$$K_7=\begin{bmatrix}-10.7985 & 1.1002 & 1.4447\\ -0.3382 & -3.6239 & 1.7432\\ -0.0346 & 3.1255 & 1.4493\end{bmatrix}$$

$$F_{18}=\begin{bmatrix}1.7048\times10^{4} & -1.4395 & 2.5521\\ -2.7684 & 1.6717\times10^{4} & 125.5132\\ -1.4906 & 119.8547 & 1.6940\times10^{4}\end{bmatrix}$$

$$K_8=\begin{bmatrix}-10.8124 & -0.5334 & 1.3669\\ 0.8643 & -3.6101 & 1.7569\\ -0.0868 & 3.1391 & 1.4493\end{bmatrix}$$

For a fair comparison, the same simulation conditions are taken. Time response of the attitude and angle velocity in the absence of actual faults are depicted in Figure 9. Figure 10 shows the faults estimation errors and attitude angle velocity estimation errors. It can be seen that, all methods could reconstruct the actuator fault values, whether the intermittent fault or fast time varying fault. The estimation errors obtained by all methods asymptotically converge to a small bounded interval. Differently, the proposed observer obtains better performance in the aspect of convergence rate and amplitude of estimation errors. Both the fault estimation errors and angle velocity estimation errors of Theorem 1 are one order of magnitude smaller than that of observers in [10] and [19]. The fault estimation errors of Theorem 2 is smaller than that of observers in Theorem1, Refs. [10] and [19].

Analysis results of the above two parts have verified the feasibility and effectiveness of the proposed Theorem 1 and 2.

5 | CONCLUSION

In this paper, based on T-S fuzzy models, we presented a novel FAFEO with AP to solve the fault estimation problem of satellite actuator subject to unknown model uncertainties and unpredictable actuator faults. The added AP not only provides additional design freedom to the FAFEO, but also enhances the fault estimation performance. The design was given in the terms of LMI, which could be easily calculated and has high numerical stability. Fault estimation results with less conservatism were obtained via the strict implicit constraint elimination and an auxiliary H_∞ index, while retaining the performance of present algorithm. The results show that the introduced quantitative descriptions are conducive to characterize and distinguish differences in fault estimation performance. Furthermore, the effect of model uncertainties was suppressed by the H_∞ method in our work. As future investigation, the developed fault estimation strategy can be extended to address the issue of anti-disturbance fault estimation of flexible satellite.

CONFLICT OF INTEREST

The authors declare that there is no conflict of interests regarding the publication of this paper.

ACKNOWLEDGEMENTS

This work was supported by the National Natural Science Foundation of China (No. 62005275). The authors greatly appreciate the above financial support.

DATA AVAILABILITY STATEMENT

The data that support the findings of this study are available from the corresponding author upon reasonable request.

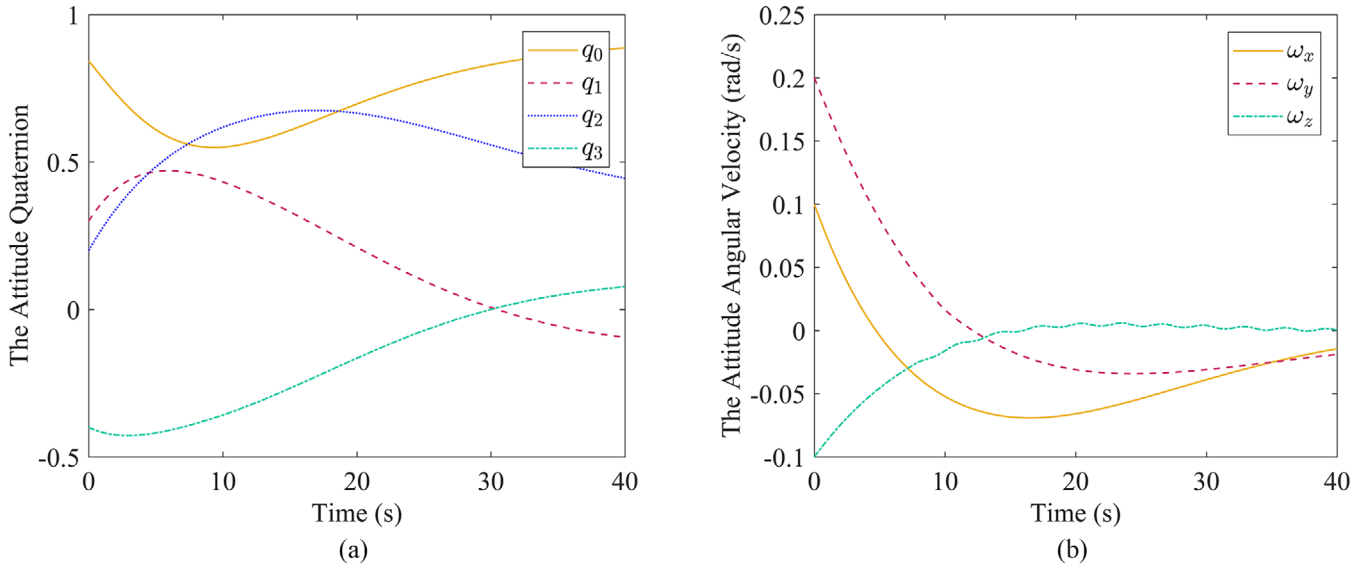

FIGURE 9 Time response of the system states: (a) the attitude(b) the angular velocity

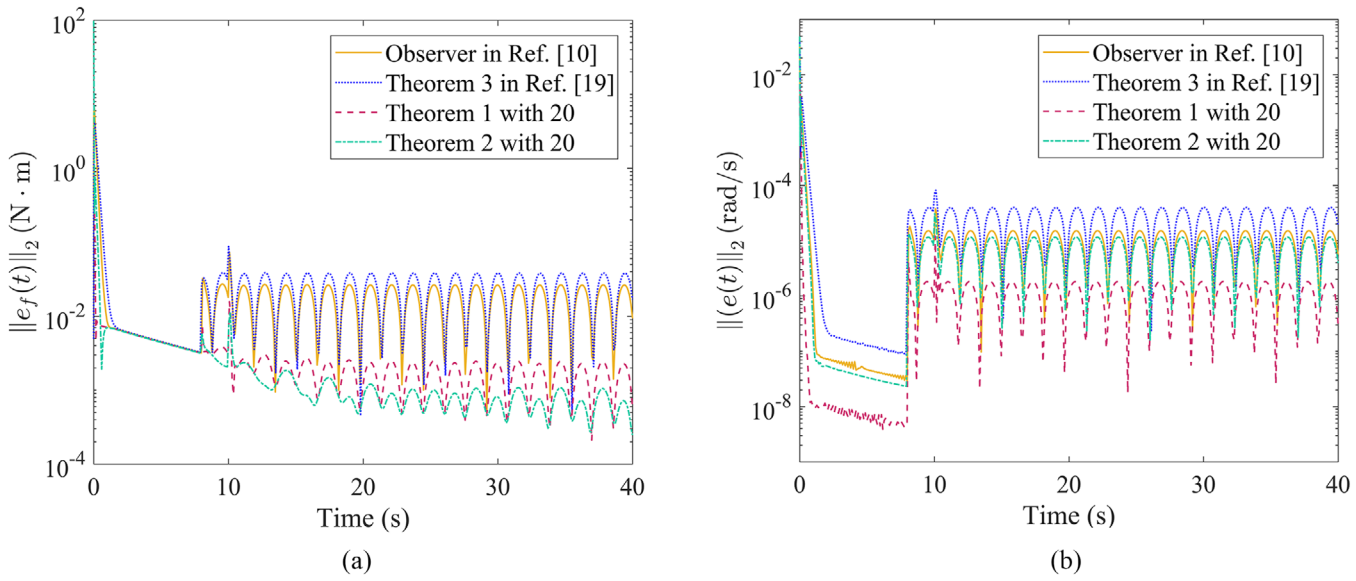

FIGURE 10 Comparison of estimation errors: (a) norm of the fault estimation error $e_f(t)$(b) norm of the angular velocity estimation error $e(t)$

REFERENCES

1. Qian, M.S., Yi, H., Zheng, Z.: Integrated fault tolerant attitude control approach for satellite attitude system with sensor faults. Optim. Control Appl. Methods 41(2), 555–570 (2020). https://doi.org/10.1002/oca.2557
2. Yin, S., Xiao, B., Ding, S.X., Zhou, D.H.: A review on recent development of spacecraft attitude fault tolerant control system. IEEE Trans. Ind. Electron. 63(5), 3311–3320 (2016). https://doi.org/10.1109/tie.2016.2530789
3. Shen, Q., Wang, D.W., Zhu, S.Q., Poh, E.K.: Robust control allocation for spacecraft attitude tracking under actuator faults. IEEE Trans. Control Syst. Technol. 25(3), 1068–1075 (2017). https://doi.org/10.1109/tcst.2016.2574763
4. Cai, W.C., Liao, X.H., Song, Y.D.: Indirect robust adaptive fault-tolerant control for attitude tracking of spacecraft. J. Guid. Control Dyn. 31(5), 1456–1463 (2008). https://doi.org/10.2514/1.31158
5. Baldi, P., Blanke, M., Castaldi, P., Mimmo, N., Simani, S.: Fault diagnosis for satellite sensors and actuators using nonlinear geometric approach and adaptive observers. Int. J. Robust Nonlinear Control 29(16), 5429–5455 (2019). https://doi.org/10.1002/rnc.4083
6. Lan, J.L.: Asymptotic estimation of state and faults for linear systems with unknown perturbations. Automatica 118, 5 (2020). https://doi.org/10.1016/j.automatica.2020.108955
7. Jmal, A., Naifar, O., Ben Makhlouf, A., Derbel, N., Hammami, M.A.: Adaptive estimation of component faults and actuator faults for nonlinear one-sided lipschitz systems. Int. J. Robust Nonlinear Control 30(3), 1021–1034 (2020). https://doi.org/10.1002/rnc.4808
8. Wang, H., Daley, S.: Actuator fault diagnosis: An adaptive observer-based technique. IEEE Trans. Autom. Control 41(7), 1073–1078 (1996). https://doi.org/10.1109/9.508919

9. Jiang, B., Staroswiecki, M., Cocquempot, V.: Fault accommodation for nonlinear dynamic systems. IEEE Trans. Autom. Control 51(9), 1578–1583 (2006). https://doi.org/10.1109/tac.2006.878732
10. Yang, P., Ma, B., Dong, Y., Liu, J.W.: Fault-tolerant consensus of leader-following multi-agent systems based on distributed fault estimation observer. Int. J. Control Autom. Syst. 16(5), 2354–2362 (2018). https://doi.org/10.1007/s12555-017-0223-y
11. Li, M., Liu, M., Zhang, Y.C., Cao, X.B.: A novel sth-order observer for linear system: Application to state and fault estimation of spacecraft control system. Int. J. Robust Nonlinear Control 29(1), 209–223 (2019). https://doi.org/10.1002/rnc.4397
12. Thakur, D., Srikant, S., Akella, M.R.: Adaptive attitude-tracking control of spacecraft with uncertain time-varying inertia parameters. J. Guid. Control Dyn. 38(1), 41–52 (2015). https://doi.org/10.2514/1.G000457
13. MacKunis, W., Leve, F., Patre, P.M., Fitz-Coy, N., Dixon, W.E.: Adaptive neural' network-based satellite attitude control in the presence of cmg uncertainty. Aerosp. Sci. Technol. 54, 218–228 (2016). https://doi.org/10.1016/j.ast.2016.04.022
14. Fazlyab, A.R., Saberi, F.F., Kabganian, M.: Adaptive attitude controller for a satellite based on neural network in the presence of unknown external disturbances and actuator faults. Adv. Space Res. 57(1), 367–377 (2016). https://doi.org/10.1016/j.asr.2015.10.026
15. Rabaoui, B., Rodrigues, M., Hamdi, H., Braiek, N.B.: A model reference tracking based on an active fault tolerant control for Lpv systems. Int. J. Adapt. Control Signal Process. 32(6), 839–857 (2018). https://doi.org/10.1002/acs.2871
16. Brahim, I.H., Chaabane, M., Mehdi, D.: Fault-tolerant control for T-S fuzzy descriptor systems with sensor faults: An Lmi approach. Int. J. Fuzzy Syst. 19(2), 516–527 (2017). https://doi.org/10.1007/s40815-016-0154-4
17. Lan, J.L., Patton, R.J.: A decoupling approach to integrated fault-tolerant control for linear systems with unmatched non-differentiable faults. Automatica 89, 290–299 (2018). https://doi.org/10.1016/j.automatica.2017.12.011
18. Liu, M., Zhang, L.X., Zheng, W.X.: Fault reconstruction for stochastic hybrid systems with adaptive discontinuous observer and non-homogeneous differentiator. Automatica 85, 339–348 (2017). https://doi.org/10.1016/j.automatica.2017.07.071
19. Zhang, K., Cocquempot, V., Jiang, B.: Adjustable parameter-based multi-objective fault estimation observer design for continuous-time/discrete-time dynamic systems. Int. J. Control Autom. Syst. 15(3), 1077–1088 (2017). https://doi.org/10.1007/s12555-015-0383-6
20. Zhang, K., Jiang, B., Shi, P.: Distributed fault estimation observer design with adjustable parameters for a class of nonlinear interconnected systems. IEEE Trans. Cybern. 49(12), 4219–4228 (2019). https://doi.org/10.1109/tcyb.2018.2860588
21. Li, X.J., Yang, G.H.: Robust adaptive fault-tolerant control for uncertain linear systems with actuator failures. IET Control Theory Appl. 6(10), 1544–1551 (2012). https://doi.org/10.1049/iet-cta.2011.0599
22. Golabi, A., Beheshti, M., Asemani, M.H.: H-infinity robust fuzzy dynamic observer-based controller for uncertain Takagi-Sugeno fuzzy systems. IET Control Theory Appl. 6(10), 1434–1444 (2012). https://doi.org/10.1049/iet-cta.2011.0435
23. Tavasolipour, E., Poshtan, J., Shamaghdari, S.: A new approach for robust fault estimation in nonlinear systems with state-coupled disturbances using dissipativity theory. ISA Trans. 114, 31–43 (2021). https://doi.org/10.1016/j.isatra.2020.12.040
24. Lee, D., Leeghim, H.: Reaction wheel fault-tolerant finite-time control for spacecraft attitude tracking without unwinding. Int. J. Robust Nonlinear Control 30(9), 3672–3691 (2020). https://doi.org/10.1002/rnc.4957
25. Fazeli, S.M., Abedi, M.: An integrated fault estimation and fault tolerant control method using H-infinity-based adaptive observers. Int. J. Adapt. Control Signal Process. 34(9), 1259–1280 (2020). https://doi.org/10.1002/acs.3144
26. Jiang, B., Zhang, K., Liu, C., Yang, H.: Fault diagnosis and accommodation with flight control applications. J. Control Decis. 7(1), 24–43 (2020). https://doi.org/10.1080/23307706.2019.1686434
27. Youssef, T., Chadli, M., Karimi, H.R., Wang, R.: Actuator and sensor faults estimation based on proportional integral observer for ts fuzzy model. J. Franklin Inst. Eng. Appl. Math. 354(6), 2524–2542 (2017). https://doi.org/10.1016/j.jfranklin.2016.09.020
28. Hu, Q.L., Niu, G.L., Wang, C.L.: Spacecraft attitude fault-tolerant control based on iterative learning observer and control allocation. Aerosp. Sci. Technol. 75, 245–253 (2018). https://doi.org/10.1016/j.ast.2017.12.031
29. Chen, W., Saif, M.: Observer-based fault diagnosis of satellite systems subject to time-varying thruster faults. J. Dyn. Syst. Meas. Control Trans. Asme 129(3), 352–356 (2007). https://doi.org/10.1115/1.2719773
30. Zhang, J., Swain, A.K., Nguang, S.K.: Robust sensor fault estimation scheme for satellite attitude control systems. J. Franklin Inst. Eng. Appl. Math. 350(9), 2581–2604 (2013). https://doi.org/10.1016/j.jfranklin.2013.06.010
31. Gao, Z.F., Zhou, Z.P., Qian, M.S., Lin, J.X.: Active fault tolerant control scheme for satellite attitude system subject to actuator time-varying faults. IET Control Theory Appl. 12(3), 405–412 (2018). https://doi.org/10.1049/iet-cta.2017.0969
32. Anderson, N.T., Marchisio, G.B.: Worldview-2 and the evolution of the digitalglobe remote sensing satellite constellation. In: *Annual Conference on Algorithms and Technologies for Multispectral, Hyperspectral, and Ultraspectral Imagery XVIII*. Baltimore, MD (2012)
33. Xu, C., Yang, X.B., Xu, T.T., Zhu, L., Chang, L., Jin, G., Qi, X.D.: Study of space optical dynamic push-broom imaging along the trace of targets. Optik 202, 14 (2020). https://doi.org/10.1016/j.ijleo.2019.163640
34. Wang, F., Xi, R.C., Yue, C.F., Li, H.Y., Cao, X.B.: Conceptual rotational mode design for optical conical scanning imaging small satellites. Sci. China Technol. Sci. 63(8), 1383–1395 (2020). https://doi.org/10.1007/s11431-020-1667-4
35. Tanaka, K., Wang, H.O.: Fuzzy Control Systems Design and Analysis: A Linear Matrix Inequality Approach. Wiley, Hoboken, NJ (2001)
36. Tanaka, K., Ikeda, T., Wang, H.O.: Fuzzy regulators and fuzzy observers: relaxed stability conditions and lmi-based designs. IEEE Trans. Fuzzy Syst. 6(2), 250–265 (1998). https://doi.org/10.1109/91.669023
37. Kim, E., Lee, H.: New approaches to relaxed quadratic stability condition of fuzzy control systems. IEEE Trans. Fuzzy Syst. 8(5), 523–534 (2000). https://doi.org/10.1109/91.873576
38. Wang, W.J., Chen, Y.J., Sun, C.H.: Relaxed stabilization criteria for discrete-time T-S fuzzy control systems based on a switching fuzzy model and piecewise Lyapunov function. IEEE Trans. Syst. Man Cybern. Part B Cybern. 37(3), 551–559 (2007). https://doi.org/10.1109/tsmcb.2006.887434
39. Li, J., Yang, G.-H.: Fuzzy descriptor sliding mode observer design: A canonical form-based method. IEEE Trans. Fuzzy Syst. 28(9), 2048–2062 (2020). https://doi.org/10.1109/tfuzz.2019.2930036
40. Kuppusamy, S., Joo, Y.H.: Memory-based integral sliding-mode control for T-S fuzzy systems with Pmsm via disturbance observer. IEEE Trans. Cybern. 51(5), 2457–2465 (2021). https://doi.org/10.1109/tcyb.2019.2953567
41. Islam, S.I., Lim, C.-C., Shi, P.: Robust fault detection of T-S fuzzy systems with time-delay using fuzzy functional observer. Fuzzy Sets Syst. 392, 1–23 (2020). https://doi.org/10.1016/j.fss.2019.03.020
42. Xu, S.D., Wei, Z.T., Huang, Z., Wen, H., Jin, D.P.: Fuzzy-logic-based robust attitude control of networked spacecraft via event-triggered mechanism. IEEE Trans. Aerosp. Electron. Syst. 57(1), 206–226 (2021). https://doi.org/10.1109/taes.2020.3012000
43. Nemati, F., Hamami, S.M.S., Zemouche, A.: A nonlinear observer-based approach to fault detection, isolation and estimation for satellite formation flight application. Automatica 107, 474–482 (2019). https://doi.org/10.1016/j.automatica.2019.06.007
44. Hashemi, M., Tan, C.P.: Integrated fault estimation and fault tolerant control for systems with generalized sector input nonlinearity. Automatica 119, 7 (2020). https://doi.org/10.1016/j.automatica.2020.109098
45. Chan, J.C.L., Lee, T.H., Tan, C.P., Trinh, H., Park, J.H.: A nonlinear observer for robust fault reconstruction in one-sided lipschitz and quadratically inner-bounded nonlinear descriptor systems. IEEE Access 9, 22455–22469 (2021). https://doi.org/10.1109/access.2021.3056136
46. Boyd, S., Ghaoui, L.E., Feron, E., Balakrishnan, V.: Linear Matrix Inequalities in System and Control Theory. Society for Industrial and Applied Mathematics, Philadelphia, PA (1994)

47. Liu, X.D., Zhang, Q.L.: New approaches to H-infinity controller designs based on fuzzy observers for T-S fuzzy systems via Lmi. Automatica 39(9), 1571–1582 (2003). https://doi.org/10.1016/s0005-1098(03)00172-9
48. Chilali, M., Gahinet, P.: H infinity design with pole placement constraints: An Lmi approach. IEEE Trans. Autom. Control 41(3), 358–367 (1996). https://doi.org/10.1109/9.486637
49. Scherer, C., Gahinet, P., Chilali, M.: Multiobjective output-feedback control via Lmi optimization. IEEE Trans. Autom. Control 42(7), 896–911 (1997). https://doi.org/10.1109/9.599969
50. Wu, X., Luo, S.B., Wei, C.S., Liao, Y.X.: Observer-based fault-tolerant attitude tracking control for rigid spacecraft with actuator saturation and faults. Acta Astronaut. 178, 824–834 (2021). https://doi.org/10.1016/j.actaastro.2020.10.017

How to cite this article: Li, Y., Xu, W., Chang, L.: Fuzzy adaptive observer-based fault estimation design with adjustable parameter for satellite under unknown actuator faults and perturbations. IET Control Theory Appl. 16, 741–761 (2022). https://doi.org/10.1049/cth2.12267